1-1-1983

# Modulated hydrostatic transformer.

Parveen Kumar Gupta

# MODULATED HYDROSTATIC TRANSFORMER

by

Parveen Kumar Gupta

A Thesis

Presented to the Graduate Committee

of Lehigh University

in Candidacy for the degree of

Master of Science

in

Mechanical Engineering

Lehigh University

1983

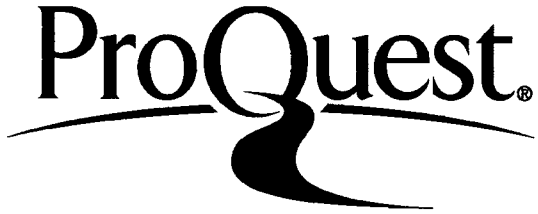

This thesis is accepted and approved in partial fulfillment of the requirements for the degree of Master of Science.

(Date)

Forbes T. Brown
Professor in charge

Fazil Erdogan
Chairman of Department

## ACKNOWLEDGMENTS

This work was supported by a grant from Parker Hannifin Corporation.

The author wishes to thank Dr. Forbes T. Brown for the interest and expertise which provided invaluable guidance for his personal and professional development. Thanks are also extended to Prof. Stanley J. Jakubowski for his very practical suggestions.

Finally, The author wishes to dedicate this work to his parents Tara and Vijay. Only with their support and understanding was the author able to reach higher ideals in life.

Table of Contents

ABSTRACT

The concept of a modulated hydrostatic transformer is proposed as an ideally non-dissipative continuous-state substitute for linear hydraulic control valves for low frequencies. This concept offers the possibility of greatly enhanced energy efficiency, especially in applications where high output pressures with low output flows occur less often than the inverse . It is analogous to the hydrostatic transmission, but with fluid inputs and outputs rather than mechanical, and with an infinitely variable displacement ratio.

Certain basic properties and design considerations are given, emphasizing the effects of leakage and mechanical and fluid friction.

A particular radial-piston design is presented, including initial experimental data on a real machine.

# 1. INTRODUCTION

Energy efficiency of hydraulic power systems recently has become of considerable interest. At the same time the microprocessor has emerged to permit more flexible control schemes than previously.

Consequent improvements in the slow-response directional control circuits, which comprise the bulk of industrial, agricultural and earth moving systems, have been made. Power supplies based on a fixed displacement pump and a relief valve are being replaced by variable displacement pumps controlled by output pressure. Excess pressure during various parts of the cycle is reduced by the use of a tandem center valve, pilot-controlled unloading valves used in conjuction with a check valve and an accumulator, or pilot-controlled relief valves which controls the supply pressure at a small margin above that produced instantaneously by the load. To virtually eliminate both the excess pressure and the excess flow at the same time, pilot operated variable displacement pumps are being used. Such load sensing circuits in general do not cope effectively with more than one load at a time, with the exception of series connected tandem center valves which unfortunately

require over-sized plumbing and valves.

Virtually all controls of a fixed-pressure or a fixed-flow hydraulic power source for non-switching systems used today employ analog valves. These valves control by modulated dissipation or resistance; thus high efficiency is impossible by definition on other than pilot flows or small regulated pressure differences. Even the pilot stages of such valves normally have a significant quiescent flow and associated steady power loss. Nevertheless, such valves are being used increasingly in the slow-response system market for the enhanced control they provide. Also, proportional servo valves form the basis of the fast-response systems needed in the robot, machine tool and aerospace industry.

Jet-pipe pilot valves inherently have low efficiency because of continuous leakage, but nevertheless their tolerance for dirt often justifies their use. The quiescent power drain alone is becoming a major liability for hydraulic as opposed to electric control.

The objective of the present research and development is to conceive and demonstrate an analog power controller based on the idea of ideally non-

dissipative continous state transformation rather than resistance. This idea virtually assumes microprocessor control.

## 2. CONCEPT

The concept of a modulated hydrostatic transformer, abbreviated as MHT herein, is proposed essentially as a continuous-state non- dissipative substitute for a linear valve to handle lower frequencies.

The vane wheel shown in Fig. 1 is a primitive prototype of the proposed modulated hydrostatic transformer. The construction is simple with the vane ring having ten slots in which the vanes are permitted to move radially only. These vanes are in constant contact with the fixed cam surface placed eccentrically with respect to the vane ring.

As the vane ring starts to rotate, the vanes move in and out radially in their respective slots. Thus the individual vanes act alternatively, every half a revolution, as a pump or as a motor. The transformation ratio varies as the center of the vane ring is displaced horizontally (i.e. eccentricity is changed). When the center of the vane wheel is moved too far from the center of the circular cam surface the fluctuations in pressure and flow become large, limiting the modulation of the transformation ratio in the range of -1 to +1 through

zero or, if the ports are interchanged, through plus or minus infinity as indicated in Fig. 1.

This design, though simple in concept and construction, suffers from two major flaws. First, at the opening or closing of ports, the volume of the chambers between successive vanes changes very rapidly causing cavitation and excessive pressure peaks. Second, excessive friction would produce either unacceptable break-away forces, or if a hydrostatic bearing is used to reduce friction, leakage might be excessive.

Thus, an acceptable and efficient design should not have rapid changes in the volume of the chambers during their periods of isolation. Also, to keep the leakage low and break-away frictional forces to a minimum, the major forces should balance one another or be supported by anti-friction bearings. Only the minor forces should be balanced hydraulically.

In the present design, an ideal analog control system would introduce an externally controllable impedence matching device which would dissipate no energy. By defination, this is called the modulated hydrostatic transformer. Servo valves, also used for

continuous state control, dissipate a large amount of energy and hence are essentially different from the MHT. By analogy, a servo valve could be called a modulated hydrostatic resistor.

The proposed arrangement has two units: pump and motor. Two ports through which the input flow enters and returns constitute the pump side with flow $Q_i$ and pressure $P_i$. The other two ports through which the load flow enters and exits is the motor end with output flow $Q_o$ and pressure drop $P_o$. By definition, an ideal transformer dissipates no energy, i.e. $P_iQ_i = P_oQ_o$. Also there would be a definite transformer ratio between the two flows and the inverse ratio between the two pressures. The word 'modulated' is used because this transformer ratio is to be controlled independently. Ideally, the ratio would vary from minus infinity to plus infinity through zero, with repetition of the cycle at infinity. An alternative possibility is tan $\theta$ or cot $\theta$, $\theta$ being the control variable.

All transformers convert energy from one form to another. As an example, in the electrical transformer, energy is converted from electrical to magnetic and back to electrical. In the proposed device, the closest

analogous energy transduction would be from hydrostatic to hydrokinetic and back. This is impractical, however.

Any pure fluid transformer in which the energy changes from hydrostatic to hydrokinetic and back would involve convertion from steady motion to oscillatory motion and back. Such a device would have low efficiency mainly due to viscosity and turbulence of the fluid, and a low power-to-weight ratio. For a practical small high-power transformer it seems inevitable that the energy would have to transform from fluid power to mechanical power and back. In short, the device would have two back-to-back variable- displacement pump/motors.

A hydrostatic transmission, or a hydraulic displacement-type transmission, is a combination of two interconnected positive displacement units - a pump and a motor [8]. One or both of these two units(i.e. the pump and the motor) has a variable displacement. It is a transformer with mechanical energy being converted to hydrostatic and back. Thus, unlike the MHT, the hydrostatic transmission has hydrostatic as the intermediate form of energy. Also, it couples a single source to a single load, whereas the MHT can couple any number of loads to a single source. Further, the loads

driven by the hydrostatic transmission are essentially rotary but those driven from the transformer can be of various types.

An assembly drawing of the proposed arrangement is given in Fig. 2 with important components and their functions as listed below. This device was conceived by the author's supervisor, F.T. Brown; the author investigated many of the details, prepared the drawings, ordered the standard parts, and directed the fabrication. The major components were machined by the Ephrata Tool Co. of Ephrata, Pennsylvania.

Major components:

1 Pintle (central stationary part) with hydrostatic bearing.

2 Rotor containing twenty pistons, ten on each center acting as pump and motor, respectively.

3 Ball bearings acting as cams.

4 Eccentric surfaces supporting the cam ball bearings.

5 Eccentrically mounted ball bearings to support the sun gear of an epicyclic gear train and the housing for the cam bearings.

6 Ball bearings to concentrically support the spider of the epicyclic gear train.

7 Spider of the epicyclic gear train.

8 Worm and the worm gear assembly for the modulation of the displacement of the pump and motor.

9 Fixed ring gear of the epicyclic gear train.

10 A pair of pinions coupling the motion of the sun gear, spider and the fixed ring gear.

11 Sun gear of the epicyclic gear train.

12 End cover with fluid inlet and outlet ports (there are two more inlet and outlet ports on the opposite side in a plane perpendicular to the section snown).

13 Cylindrical pistons with reciprocating motion.

10 Circular housing.

15 Cover plates.

## 2.1 PROPOSED RADIAL PISTON DESIGN

The present design differs from the vane wheel described above primarily in the use of radial pistons instead of vanes.

As indicated in Fig. 2 the central stationary part or pintle supports the rotor with hydrostatic bearings at two axial locations. Flow is provided to each bearing through a central hole and four radial capillary restrictions. The rotor comprises a brass sleeve in the center and a cast iron piston block, pressed together. Two pump/motors each have ten radial pistons; one such unit is pictured in Fig. 3 . Flow enters and leaves through ports in the pintle; the high pressure in both ports forces all twenty pistons outward against the cam surface (which turns about its own center since it is the race of a ball bearing).

The displacement per revolution of a pump/motor is proportional to the eccentricity of its cam surface relative to the center of the pintle. The rotor speed

thus is proportional to the eccentricity of the unit which acts as a motor and to the flow passing through the motor ports (input). The flow through the unit acting as a pump (output) is in turn proportional to the speed and its eccentricity. Thus the ratio of the flow in the output ports to the flow in the input ports equals the ratio of the two eccentricities.

It is desired that one eccentricity be proportional to Sin $\theta$ while the other is perportional to Cos $\theta$, where $\theta$ is a control variable, to give a flow ratio of tan $\theta$ or cot $\theta$ which goes from minus infinity through zero to plus infinity in a smooth way. This can be accomplished if the loci of the centers of the two cam surfaces are located on two perpendicular lines in a plane normal to the axis of the machine, as shown in Fig. 4. Further, the distance between these two centers is a constant for all $\theta$. This suggests that the two cam surfaces can be rigidly connected together in a single movable housing. The location of the housing for each angle, $\theta$, is indicated by the corresponding line segments connecting the two centers.

The desired motion of the cam surfaces is accomplished by an epicyclic gear train as pictured in

Fig. 5. The cam surface (or the outer races of the ball bearings which have the cam surfaces as their inner races) is attached rigidly to the sun gear, which thus must have the same motion. The ring gear is fixed and concentric with the axis of the pintle (i.e. the main axis of the machine). The spider, which carries two pinions forming a drive connection between the sun and ring gears, is externally rotated to give the desired position. Because the sun gear has precisely half the diameter and number of teeth of the ring gear, its rotation is precisely equal and opposite that of the spider.

Note that the center of the line segment connecting the two centers of eccentricity itself moves in a circle with a radius equal to one-half the maximum eccentricity. This is precisely accomplished by the epicyclic gear train.

The spider is positioned by a worm and worm wheel; the worm is driven by a crank external to the machine. The single-thread worm wheel has 128 teeth, so one revolution gives a change of 2.812 degrees . The ball bearings which support the spider (outside) and sun gear/cam (inside) can be seen in Fig. 2, along with the

worm assembly. Anti-friction bearings were chosen because of the large radial forces which otherwise might require excessive forces for adjustment.

## 3. DETAILED DESIGN CONSIDERATIONS

It has already been pointed out that the two major sources of inefficiency in the modulated hydrostatic transformer are leakage and the friction. To reduce leakage, one would need to decrease the clearances and/or increase the viscosity of the fluid. Decreasing the clearances would increase the probability of contaminents blocking the clearance paths, and the manufacturing cost could go up considerably. On the other hand, high viscosity would increase friction. Thus a trade-off has to made amongst the leakage, clearance and the viscosity.

### 3.1 FORCE CONSIDERATIONS

To reduce friction, one may reduce forces, balance them by proper design and/or reduce the coefficient of friction by improving the surface finish. An analysis of the more important forces that act on the various elements follows.

The major hydrostatic forces on the rotating cylinder block are balanced (the force due to pressurized fluid on the piston is balanced mainly by the fluid force acting on the cylinder block in the opposite direction). This situation may be called `hydraulic balancing'.

The minor forces acting on the rotating piston block are borne by the externally pressurized bearing pictured in Fig. 6. The outer surface of the stationary shaft or pintel has four shallow oil pads along the circumfrence [7]. These are supplied with oil under pressure through individual hydraulic resistances in the form of capillary tubes from a common pressure manifold. The oil system, consisting of an arrangement of oil pools and external resistances, will tend to compensate automatically for any misalignment of the bearing surfaces by controlling the oil flow through the capillaries and hence the pressure drops across them.

An analytical treatment to compute the dimensions of the capillary tubes (Fig. 7) and the load capacity of the bearing is as follows:

When the journal and the bearing are concentric, the total flow through all four external resistances is given by Hagen- Poiseuille law:

$$Q = 4\pi r^4(P-p)/8\mu l \qquad (3.1.1)$$

The total flow through the concentric bearing is:

$$Q = 4Rc^3 p\pi/12\mu L \qquad (3.1.2)$$

Using the principle of continuity to combine the

above two equations, one has

$$P/p = 1+4/6(R/r)(l/L)(c/r)^3 \qquad (3.1.3)$$

where r is the radius of capillary tube

$\mu$ is fluid viscocity ($1.38 \times 10^{-2}$ N.s/m$^2$)

l is length of capillary tube (0.019-0.0024 = 0.017 m)

P is the manifold pressure (20.7 MPa)

p is the pressure in the oil pads (appx. 6.9 to 10.4 MPa)

L is the length of plates (0.0064 m)

c is the radial clearance between shaft and the sleeve

R is the radius of the shaft (0.019 m)

Assuming P/p = 3, i.e. the pressure drop across the capillary is two-thirds of the manifold pressure, and a radial clearance between the shaft and the sleeve of 7.6 μm, 10.2 μm and 12.5 μm results in capillary diameters of 101.6 μm, 127 μm and 152 μm respectively. Instead, if P/p = 2, i.e. the pressure drop across the capillary tube is half of manifold pressure, capillary diameters of 127 μm, 152 μm and 178 μm respectively would result (for the same radial clearances as given above).

It was decided to have capillaries with a diameter of 152 μm and P/p = 2, resulting in a radial clearance of 10.2 μm.

For load capacity computations refer to Fig. 6. The external load is

$$W = (P_3-P_1)(A+A_1/2) \qquad (3.1.4)$$

where A is the projected area at full pool pressure

$A_1$ is the projected area of the region having linear pressure gradient

$P_3$ and $P_1$ are upper and lower pressures respectively.

The above equation can be reduced to

$$W = P(A+A_1/2)F_w \qquad (3.1.5)$$

where $F_w$ is the load factor and

P is the manifold pressure.

For a manifold pressure of 20.7 MPa, a pressure pad width of 0.0064 m and a total bearing length of 0.019 m, and assuming that the pressure in a given pool extends circumfrencially over a complete quadrant, one would need to know $F_w$ to compute W. The load factor, $F_w$, can be computed from a graph between the load factor and the attitude [7]. An attitude of n = 0.5, P/p = 2 and $F_w$ =

0.2 gives about 5115 N as the load capacity, which is quite significant.

Various forces acting on the piston are discussed in section 3.3.

Major forces on the relatively fixed control parts are borne by three pairs of ball bearings. As an example, consider the selection of the inner pair of ball bearings. The radial pistons, which are under the action of fluid pressure on one end, are in contact with the inner race of the ball bearing at the cap end. For an inlet pressure of 20.7 MPa and a piston diameter of 0.0127 m, the net force acting on the piston is $20.7(0.0127)^2\pi/4 = 2650$ N, which hereafter is called the `contact force'.

There are two principal modes of operation:

mode 1 : The lower pressure at the two output ports is essentially atmospheric. This implies a sump in the output loop, and unless fancy valving is incorporated the the output flow must be unidirectional to prevent cavitation.

mode 2: One of the output pressures is held neld constant or regulated at an elevated

pressure. This permits significant forward and reverse flows and pressure drops without cavitation. The losses are not symmetric, however, and are greater than in mode 1.

For the reason of simplicity, most analysis done here assumes the first mode of operation i.e. the output from the motor end is at atmospheric pressure. The experiment, however, employs the second mode with the fixed output pressure set at the supply pressure for the input side. Predictions of losses etc. can be converted from one mode to the other using the model of Cnapter 4.

At all times, only five pistons at each center are under high pressure, the remaining five being at the atmospheric pressure. Thus the total radial force on each center is approximately 13250 N. which is well within the load capacity of the prescribed Kaydon bearing KF050XPO. Similarly the other two pairs of ball bearings are also selected.

The Torrington bearing catalog [9] indicates that the coefficient of friction for roller bearings is of the

order of $2x10^{-3}$. Assuming the same coefficient of friction for ball bearings, the net force of 13250 N. gives a net frictional force of $13250x2x10^{-3}$ = 26.5 N. If the inner race rotates at 30 rps corresponding to a linear velocity of $0.152x\pi x30$ = 14.36 m/s (the diameter here has been approximated to 0.152 m), the power loss due to rolling friction becomes 26.5x14.36 = 380.5 W which could be tolerated.

The bearing race will move approximately at the average velocity of the ten pistons at their points of contact. These velocities are not the same, however, due to the eccentricity. Consequently a sinusoidal relative displacement occurs, with an amplitude equal to the eccentricity. This produces frictional losses. For a contact force between the piston and the bearing of 2650 N, and an eccentricity of 0.0064 m, the total sliding distance is 0.0127 m for the half-revolution for which the piston is under maximum pressure. For a coefficient of sliding friction of $\mu$, the net frictional force for all twenty pistons (of which only ten are under high pressure) is $F = 2650x\mu x10 = 26500\mu$ N. The corresponding power loss would be of the order of $26500\mu x0.0127x30 = 10096.5\mu$ Watts. The coefficient of sliding friction

could be reasonably approximated to 0.2, giving a net power loss of 2020 W, which is quite significant. The losses are greater, of course, if the pressures in the motor outlet or the pump inlet are not small.

To avoid sliding between piston and the bearing, one could machine the inner race of the bearing with a small taper or introduce a tapered ring between the piston and the bearing. This causes the piston to rotate, hopefully, which might have the added benefit of a hydrodynamic bearing action between the piston and the cylinder. This concept was not used, in favour of non-rotating pistons with cylinderical rather than spherical caps, but is discussed in Appendix A as a possible improvement.

Consider the following two cases: (1) Piston is quite concentric inside the bearing. This corresponds to fluid lubrication conditions. (2) Piston touches the walls of the cylinder and induces dry friction.

For the case (1), the viscous losses are due to linear motion of the piston. This is equivalent to the case of steady flow between stationary and moving flat parallel plates. The shear stress on the moving plate is

given by [1]

$T_u = -b/2dp/dx-\mu v/b$ (3.1.6)

where $T_u$ is shear stress on upper plate ($N/m^2$)

b is passage width (7.6 um)

p is fluid pressure in $N/m^2$

x is distance along the passage in m.

v is piston velocity in m/s.

$\mu$ is fluid viscosity ($1.38x10^{-2}$ $N.s/m^2$)

In the present analysis each piston has a simple reciprocating motion. Between the piston and the cylinder is the fluid film. For a stroke of 0.0127 m the piston would move 0.0254 m for each revolution of the shaft. Assuming a shaft speed of 30 rps, the piston would have a linear velocity V of 0.762 m/s. Half of the pistons have a pressure drop of 20.7 MPa and for the other half there is very little pressure drop giving an average value of 10.4 MPa for each piston. The average distance along which this pressure drops is 0.0238 m. These numbers give a net shear stress of 3035 $N/m^2$ acting on an area of $\pi x0.0127x0.0238 = 0.00095$ $m^2$. Hence the total power loss for each piston is 3035x0.0095x0.762 = 2.24 W. Thus the total power loss for all twenty pistons is 45 W.

For the viscous frictional case it has been assumed tnat the piston is centered so there is no metal-to-metal contact between the piston and the cylinder. This often is not the case. When the piston touches the walls of the cylinder a higher coefficient of friction results.

The power loss due to dry friction between piston and cylinder can however be computed as follows: Consider the operation of each individual piston. As done previously, the contact force can be approximated as $20.7x(0.0127)^2\pi/4$ = 2650 N. At the point where the piston touches the walls of the cylinder, the frictional resistance and the load both are acting (their ratio being equal to the coefficient of friction). Assuming a nominal value of 0.2 for the coefficient of friction and Fcos $\theta$ as the normal force, one gets a frictional force of the order of 0.2Fcos $\theta$ . For a maximum value of cos $\theta$ = 1.0, this frictional force is of the order of 534 N. For a stroke of 0.0127 m, the piston's linear velocity would be 0.762 m/s, resulting in net power loss of 534x0.0762 = 403 W for each piston at a speed of 1800 rpm. The average power loss for each piston would be $1/\sin^2 \theta \, d\theta = 1/\pi \, x \, \pi/2 = 1/2$ of the total power loss. Thus the average power loss for each piston is 201.5 W. If at any time ten pistons are under such condition, a net loss

of 2015 W. occurs. Normalizing it with respect to maximum Normalizing it with respect to maximum power (max. flow.max. pressure = $315.5 \times 10^{-6}$ $m^3/s \times 20.7$ MPa), one gets 201.5/6530.8 = 0.03.

## 3.2 SYSTEM LEAKAGES

The leakage, which cause major losses in efficiency occur mainly at three locations in the present design:

(a)The hydrostatic bearing used to reduce friction causes the greatest leakage. The bearing is supplied with fluid at the system pressure and eventually the fluid drains out at atmospheric pressure. Thus, all the power of the fluid flowing through the bearing is lost. The total flow Q through one concentric bearing (Fig. 6) is given by [7]:

$$Q = 4\pi r c^3 p / 12 L \mu \qquad (3.2.1)$$

where P indicates manifold pressure (20.7 MPa)

p is pressure in any of the four pads (appx. 10.4 MPa)

$\mu$ is fluid viscosity ($1.38 \times 10^{-2}$ $N.s/m^2$)

c is mean radial clearance (10.2 um)

L is length of flow path in the journal (0.0064)

of 2015 W. occurs. Normalizing it with respect to maximum Normalizing it with respect to maximum power (max. flow.max. pressure = $315.5 \times 10^{-6}$ $m^3/s \times 20.7$ MPa), one gets 201.5/6530.8 = 0.03.

### 3.2 SYSTEM LEAKAGES

The leakage, which cause major losses in efficiency occur mainly at three locations in the present design:

(a)The hydrostatic bearing used to reduce friction causes the greatest leakage. The bearing is supplied with fluid at the system pressure and eventually the fluid drains out at atmospheric pressure. Thus, all the power of the fluid flowing through the bearing is lost. The total flow Q through one concentric bearing (Fig. 6) is given by [7]:

$$Q = 4\pi r c^3 p / 12 L \mu \qquad (3.2.1)$$

where P indicates manifold pressure (20.7 MPa)

p is pressure in any of the four pads (appx. 10.4 MPa)

$\mu$ is fluid viscosity ($1.38 \times 10^{-2}$ $N.s/m^2$)

c is mean radial clearance (10.2 um)

L is length of flow path in the journal (0.0064)

r is radius of the bearing (0.019 m)

The present design assumes bearing action at two places and hence the total leakage would be twice that indicated above. Using the values above, one gets a total leakage of $4.9 \times 10^{-6}$ $m^3/s$

(b) The second source of leakage is the clearance space between the central stationary member (pintle) and the rotating sleeve around the inlet ports. The design assumes an axial length of 0.0064 m in which the pressure drops linearly from system pressure to approximately atmospheric pressure at the groove. Flow through this clearance space can be estimated using the analysis for steady flow between stationary and moving flat parallel plates as depicted in Fig. 9 [1]. The result is

$Q = \{-b^3/12\mu \cdot dp/dx + vb/2\}w$ (for $w >> b$ only)

where b is radial clearance between shaft and sleeve (10.2 um)

$\mu$ is fluid viscosity ($1.38 \times 10^{-2}$ $N.s/m^2$)

w is passage width ( x0.0381 m)

v is linear velocity (30x0.0381 m/s)

(assuming a nominal sleeve speed of 30 rps)

dp/dx is mean pressure drop/unit length

(10.4 MPa/0.0064 m)

To account for total leakage, this result must be multiplied by four (two paths for each set of ports, one on either side). All these quantities lead to a total leakage of $3.8 \times 10^{-6}$ $m^3/s$.

(c)The third important source of leakage is the clearance space between each piston and its cylinder. Once again this could be computed using the above analysis for steady flow between moving and stationary flat parallel plates. Assuming concentricity,

$Q = \{-b^3/12\mu \cdot dp/dx + vb/2\}w$ (for $w >> b$)

where b is radial clearance (7.6 um)

w is width of section ( x0.0127 m)

v is linear velocity (30x0.0127 m/s)

dp/dx is average pressure drop/unit length

(10.4 MPa/0.0254 m)

Such leakage would occur in all twenty pistons. Thus, for net leakage, the result has been multiplied by twenty, resulting in a total leakage of $3.3 \times 10^{-6}$ $m^3/s$. Further, the leakage is twice this value if the pistons are in line contact with the cylinder wall.

The above mentioned three prime sources of fluid leakage add up to approximately $12.0 \times 10^{-6}$ $m^3/s$ (for the

concentric case) and the corresponding power loss at system pressure of 20.7 MPa is 250 W. This power loss is one of the main sources of inefficiency, and would appear in the form of heat.

## 3.3 PISTON SHAPE

The radial pistons which move inside the cylinder block are one of the most critical components of the modulated hydrostatic transformer. Forces acting on the piston can be classified according to the direction of action as peripherial, lateral and axial. The first class is important only when the pistons are designed to rotate (Appendix A). Lateral forces are not directly important since they act normal to the direction of motion of the piston, but indirectly tney cause axial friction forces which contribute greatly to the system losses. In some cases this friction may be so large that tne piston becomes immovable; the name `hydraulic lock' is often applied to this phenomenon. The total axial force wnich include the inertial and the frictional forces are normally quite large and hence they directly determine the design of piston operating devices [1].

LATERAL FORCES

Following is an analysis of the lateral forces in

the case of a cylindrical piston as used in the present design. Lateral force computations for some more complicated piston shapes are included in Appendix B.

Consider a simple but important problem with perfectly round piston and cylinder with axes that are parallel but not coincident [1]. The flows $dq_1$ and $dq_2$ pass tnrough two elements of peripheral clearance at the top and bottom of the piston are shown in Fig. 10, for piston being displaced upward. Each element has a peripheral width $dz = ad\theta$, normal to the plane of the figure; peripheral flow is neglected.

Since for each elementry conduit the cross sectional area $y_1dz$ or $y_2dz$ is constant over the length, 1, of the piston land, the pressure gradient $dp/dx = (P_1-P_2)/1$ is constant for both conduits. Thus the curve of pressure vs. distance is a straight line between the points $P_1$ and $P_2$. $P_1$ and $P_2$ are the pressures in the two conduits at ends of the piston. The downward force on the piston is $df_1 = Pdzdx = (P_1+P_2)1dz/2$. The upward force, $df_2$, is exactly the same; thus the two df's balance all around the piston and the net lateral force is zero for any case in which the surface of the piston is parallel with the adjacent wall of the cylinder.

Thus, tneoretically, no net lateral force exists, and consequently simple design involving cylindrical pistons is attractive. Practical problems occur, nevertheless, including valve sticking and excessive friction. As shown in Fig. 12, a dirt particle trapped in the clearance space causes a compressive force on the particle, trapping it worse and causing possibly very large axial friction forces. The force also produces a moment on the piston. These decentering forces can be greatly alleviated by the use of a fine in-line filter.

Use of a double-tapered piston can prevent metal-to-metal contact, greatly reducing frictional losses, as discussed in Appendix B. Tnis would be very expensive, however, so ultimately it was decided to use cylinderical pistons.

The pump/motor of the MHT were chosen to be of the radial piston type. Ten pistons for each of the pump and the motor have a nominal diameter and stroke of 0.0127 m.

The diameteral clearance between the piston and the cylinder was chosen to give a maximum leakage. Consider the case of a straight piston moving inside a straight

cylinder with a radial clearance of b. Assuming a net maximum allowable leakage of $3.15*10^{-6}$ $m^3/s$ from all twenty pistons [7], one has

$$Q = \pi P w b^3 / 12 L \mu \qquad (3.3.1)$$

where P is the average pressure drop (10.4 MPa)

$\mu$ is fluid viscosity ($1.38 \times 10^{-2}$ $N.s/m^2$)

L is the average piston length supporting pressure drop (0.0238 m)

w is widtn of flow passage ($\pi$x0.0127 m)

b is the breadth of the flow passage

Q is tne flow rate ($3.15 \times 10^{-6}$ $m^3/s$)

Using the various numbers, one gets an average radial clearance of 7.6 $\mu$m

The length of the pistons in the present design was chosen largely to ensure that the length of the leakage path would always be at least one diameter. A shorter length could cause excessive cocking and consequent friction as well as excessive leakage or unacceptably small clearances. The overall length, considering the constraint of available ball bearings, turned out to be 0.0309 m.

The pistons are flat on the end where fluid pressure

acts. Tne end which is in constant contact with the inner race of the bearing has a cylinderical cap. This gives line contact between the piston and the inner race of the bearing. The radius of curvature at the cylinderical end was decided in the following way:

Under normal operating conditions the following forces are acting on the piston. The contact force between the piston cap and the inner race of the ball bearing and the corresponding frictional force. Fluid pressure force acts on the flat surface of the piston. Because of the oil present in the clearance space between the piston and the cylinder, two normal forces and hence two frictional forces act on the piston. These two forces give a net moment which prevents cocking of the piston.

The center of curvature of the cylindrical cap of the piston should be so chosen that the resultant of the above four forces passes through it.

## 4. SYSTEM MODELLING

The mathematical description of the dynamic chracteristics of a system is called a mathematical model or simply a model. In deriving a reasonable model, one has to compromise between simplicity and accuracy [5].

A steady-state equivalent circuit model for the proposed mechanical system may be drawn as indicated in Fig. 12a. Leakage paths can be added between each of the two input terminals and the two output terminals.

The simplest type of operation would set the lower output pressure on the motor side, the output pressure on the pump side and the case drain pressure equal to the reservoir pressure, which would be taken as zero. Also, the series resistance, which represents porting losses, would be neglected. These two assumptions result in a simplified circuit model of Fig. 12b. The various losses are the leakages due to the supply pressure $P_s$ and the output pressure $P_o$, viscous drag and Coulomb type dry friction. Computation of the various losses follows.

### 4.0.1 Leakage at pressure $P_s$

At system pressure, leakage at three places can be identified. The locations are: (a) Fluid flow through the pressurized bearing is kind of a leakage loss. As indicated in section 3.2, this can be computed as

$Q = 8rc^3P/3L\mu(p\pi/4P)$

Substituting the various values, the net loss is $4.9x10^{-6}$ $m^3/s$. (b) Fluid leakage through the clearance space around the ports. This is the case of leakage between two parallel plates, one of which is moving and the other is fixed. As already computed in section 3.2this loss is of the order of $0.9x10^{-6}$ $m^3/s$. (This loss is half of that computed in section 3.2 since only high pressure operation is considered here). (c) The last major kind of leakage is through the clearance space between piston and cylinders. Once again as indicated in section 3.2 for all ten pistons at the system pressure this loss is of the order of $1.16x10^{-6}$ $m^3/s$.

Consider the operation of modulated hydrostatic transformer. The input power to MHT, which is product of input flow and pressure, is indicated by $Q_iP_i$. the output from MHT, again in terms of fluid power , would similarly be product of output flow $Q_o$ and pressure $P_o$.

The input pressure, $P_i$, would in general be a variable, but could be maintained constant at $P_s$ with the use of a regulated source or a large accumulator. Also, $Q_s$ is nominal refrence flow which could also be considered as the maximum steady supply flow. For most of the cycle $Q_o$ would be less than $Q_s$; but due to the accumulator for short instances it could be more than $Q_s$.

The steady pressure $P_s$ and flow $Q_s$ can be used to normalize pressure and flow and the ratio $R_n = P_s/Q_s$ as the normalizing resistance. Assuming $Q_s = 315.5 \times 10^{-6}$ $m^3/s$, one could get the above mentioned normalized leakages as 0.016, 0.006 and 0.005 respectively. Thus, the total normalized leakage flow is appx. 0.027.

### 4.0.2 Leakage at Pressure $P_o$

Again, it is made up of leakages around the clearance space and around the pistons, which add up to a normalized leakage of 0.012 as indicated above.

Viscous losses occur mainly at two locations: between the piston and the cylinder and in the annular space between the central stationary member (or pintle) and the sleeve.

In section 3.1, various losses between piston and cylinder were discussed. The net loss due to reciprocating motion of the piston inside the cylinder was 45W.

The viscous power loss due to the presence of fluid film between rotating sleeve and stationary shaft can also be estimated using following formulation [1]

$T_u = -b/2 \cdot dp/dx - \mu v/b$

where $T_u$ is shear stress acting on the piston surface ($N/m^2$)

b is radial clearance between shaft and the sleeve (10.2 um)

$\mu$ is fluid viscosity ($1.38 \times 10^{-2}$ $N.s/m^2$)

v is velocity of sleeve (1.143 m/s)

dp/dx is pr. drop in distance dx (10.4 MPa/0.0064 m)

This results in a shear stress value of 13.1 KPa acting on an area $=\Pi \times 0.0381 \times 0.0508$ $m^2$, resulting in a net power loss of 287.2 W. Adding them togather, one gets a net power loss of 332 W which is represented by $R_f$ in the circuit diagram.

The two transformer modulii for this design are taken to be

$T_1 = \sin 0$

$T_2 = \cos 0$

giving an overall transformer ratio of tan 0 or cot 0. Practically these relations can be achieved easily; one such method being the use of ring gear and a set of spur gears as indicated in the aseembly drawing. The analysis of system is straight forward, with efficiency, n, equalling $P_oQ_o/P_iQ_i$. Using Kirchoff's laws and the definition of an ideal transformer, one could compute the load pressure and the flow ratios as

$$P_o/P_s = (\cot\theta + \frac{R_f/R_1}{\sin\theta\cos\theta}) - (\frac{R_f/R_n}{\sin\theta\cos\theta})\frac{Q_i}{Q_s} + (\frac{1}{\sin\theta})\frac{S_e}{P_s} \qquad 4.1$$

$$Q_o/Q_s = -(\frac{\cot\theta}{R_2/R_n} + \frac{\tan\theta}{R_1/R_n} + \frac{R_fR_n}{R_1R_2\sin\theta\cos\theta}) + (\tan\theta + \frac{R_f/R_2}{\sin\theta\cos\theta})\frac{Q_i}{Q_s}$$
$$-(\frac{R_n/R_2}{\sin\theta})\frac{S_e}{P_s} \qquad 4.2$$

where $R_1$ is net leakage flow at pressure $P_s$

$R_2$ is net leakage flow at pressure $P_o$

$R_f$ is net viscous drag on all moving parts

$S_e$ is Coulomb type friction partly proportional to $P_i$ and partly to $P_o$.

$R_n = P_s/Q_s$ is normalizing resistance

$T_1$ and $T_2$ are transformer modulii.

One more method of modelling a system called the 'Bond Graph' is increasingly being used [14]. The bond graph of the proposed system is shown in Fig. 12c.

## 5. EXPERIMENT and CONCLUSIONS

The MHT was instrumented and three test runs were made. The chracteristics of the machine obviously changed from the first to the third run, the frictional losses decreasing as rubbing surfaces become polished. Therefore only the results of the third run are presented, and they should be viewed as tentative. Further, the instrumentation was relatively crude compared to what is planned ( by others) for further tests, and the operating points were sparcely distributed. Nevertheless they indicate that the machine behaved at least roughly as predicted, and even closer correspondance is anticipated after it has more time to run in.

The experimental set-up is diagrammed in Fig. 13. An in-line 3-micron filter was used. DTE 25 anti-wear hydraulic fluid with specific gravity of 0.867 and viscosity of 227 SUS at 100°F was used in experiments. The case drain was oriented near the top of the device, so the internal parts were submerged in oil. The input side(motor) fluid was heated to roughly 50°C and the output side(pump) fluid to roughly 40°C. The output side was operated as a simple loop, without reservoir, with

the lower pressure maintained at the supply pressure of the input side (mode 2) by a direct connection which compensates for some of the leakage. The hydrostatic bearing also was pressurized at the supply pressure. The flows in the output loop and at the outlet of the input side were measured with rotameters with possible errors of up to about 0.2 gpm. The total internal leakage was measured with a rotameter with possible errors up to about 0.02 gpm. The three different port pressures were measured with conventional Bourdon gages with errors usually less than 10 psi but occasionally possibly up to 20 psi due to needle vibration. (All pressure gages were calibrated by the author.) The power supply pressure and the pressure upstream of the filter were also measured tnough they do not affect the results.

The crank-operated worm drives the worm wheel through one complete revolution in 128 turns; one turn therefore corresponds to a change in the angle O of 2.8125 degrees. In the second run a hydraulic motor was used as a flow meter in the output loop; a change of angle no more than 0.2 degrees was sufficient to reverse the direction of the shaft rotation. At the other extreme the rotor stalled at an angle of 71 or 72 degrees for an input pressure drop of about 3400 KPa. Rotation

of the rotor was clearly audible, and its frequency might be readily measurable using a microphone.

The raw data is given in Table 1, and a graphical representation of the reduced data is given in Fig. 14.

The efficiencies which can be achieved are a key factor in evaluating the value of an MHT. The efficiencies demonstrated so far appear to be somewhat less than necessary to justify the expense. These efficiencies might improve significantly as the machine runs in, however. Further, some of the major frictional losses might be drastically reduced by design changes. In addition to those suggested above, the piston-cap/ball bearing combination might be replaced with hydrostatic shoe bearings. This change would have the added advantage of reducing the size and cost of the machine.

An overall evalution of effectiveness should include a study of the effect of various load cycles. This will require extensive use of the analytical model given herein with corrections to handle non-zero refrence pressures.

As a first step, better and more extensive data

should be taken and compared against the model.

## 6. BIBLIOGRAPHY

1. Blackburn, J. F., Reethof, G. and Shearer, J. L. Fluid Power Control. MIT press and John Wiley & Sons, Inc. 1960.

2. Ling, F. F., Klaus, E. E. and Fein, R. S. Boundary Lubrication (An appraisal of world literature) ASME, 1969.

3. Martin, H. R. Bond Graph - A Teaching Tool The Journal of Fluid Control,vol. 54 (1981) pp. 43-59.

4. McCloy, D. and Martin, H. R. Control of Fluid Power (2nd. edition) Ellis Harwood Ltd., 1980.

5. Ogata, Katsuhiko. Modern Control Engineering. Prentice-Hall,Inc., 1970

6. Paynter, H. M. Analysis and Design of Engineering Systems MIT press, 1961.

7. Shaw, M. C. and Macks Fred. Analysis and Lubrication of Bearing, MaGraw-Hill publication, 1949.

8. Stewart, H. L. Pneumatics and Hydraulics,

Theodore Audel & Co. 1980.

9. Torrington Bearing Catalog No. 567.

10. Wilson, R. E and Barnard, D. P. Mechanism of Lubrication. Journal of the Society of Automotive Engineers, vol. 11 (1922), pp.49-60.

# 7. APPENDIX A

In section 3.1 on force computations it is noted that considerable power is lost because of the relative oscillatory sliding of each piston against the inner race of the ball bearing. One way to avoid most of this sliding would be to replace the cylindrical caps on the pistons with spherical caps with the same radius of curvature, and in addition taper the inner race of the ball bearing or introduce a tapered ring between the piston and the bearing as shown in Fig. 15. The result is that the piston can rotate a few turns in each direction for each turn of the piston block, replacing sliding contact with rolling contact. Also, the rotation makes a hydrodynamic journal bearing action possible between each piston and its cylinder.

Tne taper also would produce an axial force on the cylinder block which in general is not balanced, requiring axial anti-friction or hydrostatic bearings for efficient operation. This added complexity ultimately led to abandonment of the concept in the prototype machine.

A large taper would give a large moment about the

piston axis to encourage rotation, but also a relatively small angular velocity that would discourage the desired hydrodynamic action. Thus a compromise exists. In the present case the achievement of the desired behavior was only marginally indicated, further mitigating against use of the concept. The best taper appears to be about 4 degrees which gives a contact point 0.0015 m from the center

For the journal bearing action between the piston and the cylinder, the Sommerfield number, which is an important parameter in the journal bearing theory, can be computed from its defination [2]:

$$S = (r/c)^2 N\mu/P \qquad (A.1)$$

where r is the radius of the journal (0.0064 m)

c is the radial clearance between bearing and journal (7.6 μm)

μ is oil viscosity ($1.38 \times 10^{-2}$ N.s/m$^2$)

N is the speed of piston rotation in rps (30x1.8)

P is load/unit projected bearing area

Here a speed factor of 1.8 and a nominal speed of 1800 rpm has been assumed. Note that for a contact force of 2650 N, the load P can be estimated as 450 N. The

projected bearing area would be product of the piston diameter and the piston length supporting the pressure drop, i.e. $\pi$*0.0127x0.0238 $m^2$. Using all the above quantities one would get a Sommerfield number of 0.506.

Refer to the curve which gives varition of Sommerfield number with the coefficient of friction and bearing parameters [2]. The critical point which seperates boundary lubrication from thick film lubrication has S = 0.05. Thus all values with S greater than or equal to 0.05 would correspond to a thick film lubrication and hence a lower value for the coefficient of friction. The above Sommerfield number corresponds to thick film lubrication.

Assuming that at worst one operates at the critical value of S = 0.05, the corresponding value of (r/c)f is 3.0. For r/c = 0.0064/0.0000064 = 1000, the resulting coefficient of friction f = 0.003. The net force at each center has already been approximated to 13250 N for each piston. Therefore the net frictional force on each piston is 1325x0.003 = 4 N.

Computation for the total available force can be done using Petroff's equation [7] which is valid for a

lightly loaded bearing with constant viscosity of oil across the film. Petroff's equation gives a linear variation of Sommerfield number S with (r/c)f. Extrapolating the curve for Petroff's theory [7], the calculated value of S = 0.506 would correspond to (r/c)f = 11.88, giving the coefficient of friction f = 11.88/1000. By definition, the coefficient of friction, f, is the ratio between the frictional force and the normal force [10]. Using an approximate value of 1325 N at each center for nominal force, the frictional force for each piston would be 11.88x1325/1000 = 15.75 N.

Comparing the two results, the available force is greater than the resisting force indicating that piston rotation is possible.

Once it is decided to allow the pistons to rotate, one can compute the power loss due to the various forces present between the piston and the cylinder as a function of the stroke of the piston and the pressure.

Due to piston rotation there would be an additional viscous frictional loss. For the case of a lightly loaded bearing operating in the concentric position and assuming a constant viscosity across the oil film, the

frictional force is [7]

$$F = (2\pi r L_b)\mu(2\pi r N_m/60c) \qquad (A.2)$$

where r is journal radius (0.0064 m)

$L_b$ is bearing length (0.0238 m)

u is fluid viscosity ($1.38 \times 10^{-2}$ N.s/$m^2$)

c is the radial clearance (7.6 μm)

$N_m$ is the journal speed in rpm (1800x1.8)

(It is assumed here that shaft has a nominal speed of 1800 rpm and speed factor of 1.8)

The corresponding power loss would be

$$H = F(2\pi^2 r N_m/60) \qquad (A.3)$$

$$H = 0.0689(r^3 L_b (N_m)^2 \mu/c)$$

Tnis gives a total power loss of 165 W for all twenty pistons.

Hence, the net power loss due to viscous friction for twenty pistons is 210 W.

As a confirmation of the rotational viscous losses one could do the following analysis:

$$f = F/W$$

where f is the coefficient of friction

F is the frictional force

W is the bearing load

As already indicated;

$F = (2\pi r L_b)\mu(2\pi r N_m)/60c)$

If P = Bearing load/unit projected area

i.e. $P = W/2rL_b$, then

$f = 2\pi^2\mu rN/cP$

where N is the speed in rev./sec.

Therefore, f = 0.01.

The coefficient of friction could also be deduced from Sommerfield number computations. The Sommerfield number for flow between the piston and the cylinder has already been calculated as 0.506. Extrapolating the Petroff's linear curve given in [7], the corresponding coefficient of friction is 0.01. Thus the result is the same.

Also, consider the speed of rotation. For a critical value of S = 0.05, all other parameters remaining the same, one gets a speed of 320 rpm. The Sommerfield number of 0.506 corresponds to a speed of 1800x1.8 rpm. Thus the critical Sommerfield number of 0.05 would correspond to a speed of 321 rpm, once again confirming the above analysis.

## 7.1 APPENDIX B

The deleterious effect of contact friction between the piston and cylinder walls has been pointed out in Chapter 3. Straight cylinderical pistons are assumed at that point. Following is an analysis of more complicated piston shapes which potentially eliminate metal-to-metal contact.

Consider first the commonly used conical shape for tne piston. It is assumed that the cylinder bore is true and the axis of piston and cylinder are parallel but not coincident as indicated in Fig. 17. Flow $dq_1$ and $dq_2$ through two elements of peripheral clearance space at the top and bottom of the piston are shown in the sketch,with the piston being displaced upwards. Each element has a peripheral width $dz = ad\theta$, normal to the plane of figure [1].

The cross sectional areas $y_1dz$ and $y_2dz$ vary along the length of the piston 1, producing a non-constant pressure gradient dp/dx. The resulting net lateral force can be computed by double integration.

For an elementry length, dx, of the conduit of peripheral width dz and neight y,

$$dp/dx = -12\mu/y^3 \cdot dQ/dz \qquad (B.1)$$

where $\mu$ is the absolute oil viscosity and

$dQ/dz$ is the flow through conduit of width dz.

If at a distance x from the large end the fluid pressure is P, then

$$P-P_1 = -12\mu dQ/dz \int_0^x y^{-3}\, dx$$

$$= -12\mu dQ/dz \int_0^x (c_1+tx/l)^{-3}\, dx$$

where t is radial taper of the piston

l is length of the piston

$c_1$ is smallest radial clearance at the large piston end

i.e. $P-P_1 = -12\mu dQ/dz[-1/2t\{1/c_1+tx/l)^2-1/c_1^2\}]$

The boundry condition is $P = P_2$ at $x = l$. If

$P_2-P_1 = -\Delta P$

then, on simplification one gets

$$P = P_1-\Delta P(c_1+t)^2/t(2c_1+t)\{1-c_1^2/y^2\} \qquad (B.2)$$

The above relation indicates that the variation of pressure with y (and hence with x) is parabolic (as $y = c_1+tx/l$). The actual deviation of this parabolic pressure curve from the linear curve of a uniform conduit depends essentially upon the taper and closeness of approach of the larger end to cylinder walls as shown in the figure.

The radial force on an elementry area, dxdz, of the piston will be Pdxdz. The total radial force on an elementry strip of width dz is thus given by

$$df/dz = P_1 l - \int_0^{\ell} \Delta P(c_1+t)^2/t(2c_1+t)\cdot(1-c_1^2/y^2)dx$$

which simplifies to

$$df/dz = P_1 l - \{(c_1+t)\Delta P l/(2c_1+t)\}$$

The total lateral force, F, on the piston is obtained by integrating df around the periphery, i.e. from 0 to 2 a. One must take into account the fact that only the component of df parallel to the displacement, b, is of interest since the normal component will cancell because of the symmetry. Therefore, the component of df parallel to b would be

$$dF = -la\{P_1 - \Delta P(c+t+b\cos\theta/2c+2b\cos\theta+t)\}\cos\theta$$

where c is the radial clearance at the large end with piston centered.

i.e. $c+b\cos\theta = c_1$.

Integrating O from 0 to $2\pi$ and using tables, the total lateral force on the piston is

$$F = \pi at\Delta P l/2b\{1-(2c+t)/(2c+t)^2-4b^2\} \qquad (B.3)$$

Since the second term in the parenthesis is greater than 1, the force will be negative, i.e. away from the larger opening, and is therefore a decentering force. Thus the

equilibrium of a tapered piston with the higher pressure applied to the larger end is unstable; the piston will be forced in contact with the wall. Conversely, if the higher pressure is applied to the smaller end, the piston will center itself in the bore.

The piston with a single tapered land would not work in practice, however, because its axis is not constrained to remain parallel to the axis of the cylinder. To avoid this it is necessary to employ at least two seperate tapered sections that together can withstand an applied moment as well as a lateral force. Such a geometry is shown in Fig. 17, in which the lands are seperated by a peripheral groove. The groove locally equalizes the pressure around the land. The tentative dimensions for the various lands were chosen in such a way that each of the three major forces passes through a point located at the intersection of the centerline of the cylinder and the plane of the groove.

It has already been shown that the net lateral force on a tapered piston of length L and radius a is

$$F = \pi a t \Delta P L / 2b\{1-(2c+t)/(2c+t)^2-4b^2\}$$

Here t is the radial taper, b is the eccentricity, c is the radial clearance at large end with piston centered

and P is the pressure drop in length L.

Consider operation where the supply pressure $P_s$ drops to $(2/3)P_s$ at the groove and to atmospheric pressure at the end of the tapered land. Consider first the tapered land between the flat piston end and the groove. For a supply pressure of 20.7 MPa, the pressure drop in this land is 6.9 MPa. Assuming a taper of 7.6 um, a length of 0.008 m, an average radial clearance of c= 6.4 um, and a displacement of b=c so that contact occurs at one point, one gets a net lateral force of 187.7 N. Similarly the net decentering force acting on the second land between the groove and the cap end also can be computed to be of the order of 587.1 N. Therefore, the maximum net lateral force is approximately 775 N. This accomodates an angle between the force on the cap and the cylinder centerline of 13 degrees, which may be adequate to prevent metal-to-metal contact.

Piston shapes with stepped lands can substitute for the tapered lands.

We consider the particular stepped piston shown in Fig. 18. The main force on the piston is the contact force between the piston and the bearing, which on

average passes through the center of curvature of the cylindrical cap. For stability the two other resultant forces must also pass through the same point. In the present tentative design with its 0.0023 m radius of curvature, this point falls on the groove location. It is assumed that the clearances in section (1) and (3) are equal and in (2) and (4) are equal, and that the clearance in section (2) is double the clearance in section (1). The consequent leakages and pressure drops would be in the ratio of eight to one (since $dp/dx = -12\mu/y^3 dQ/dz$) between the narrow and wide sections. Thus, the pressure at groove is two-thirds of the supply pressure.

An analysis to compute the net lateral force on the left part of the piston follows.

As indicated previously,

$dP/dx = -12\mu/y^3 dQ/dz$

If P is the pressure at distance x away from the larger end, then

$P-P_1 = -(12\mu dQ/dz)\int_0^x dx/y^3$.

The radial clearance c is a function of distance x and also angle $\theta$. Let the clearance be c and $c_1$ in the interval $0<x<1$ and $1<x<21$,

respectively. Assuming that x lies between 1 and 21,

$P = P_1 - 12\mu dQ/dz[1/c^3+(x-1)/c_1^3]$

The boundary conditions at x = 21 is $P = 2/3P_1$,

$P = P_1 - 1/3P_1/1(C^3+c_1^3)\cdot[1c_1^3+(x-1)c^3]$ (B.4)

The net radial force on a small element with area dxdz would be Pdxdz. The net radial force on a thin strip of width dz would be

$$dF/dz = \int_0^{2\ell} Pdx$$

Substituting for P and simplifying

$dF/dz = P_1 21 - P_1/31(c^3+c_1^3)(21^2c_1^3)$

To compute the net lateral force, one needs to integrate around the periphery of the piston ($dz = ad\theta$, $\theta$ varing from 0 to $2\pi$). Also, due to symmetry only the vertical components would contribute towards the net lateral force. Hence

$$dF = -2/3P_1 al \int_0^{2\pi} c_1^3/(c^3+c_1^3)\cos\theta d\theta$$

Here clearances c and $c_1$ are functions of $\theta$ only and may be replaced by $(c+e\cos\theta)$ and $(c_1+e\cos\theta)$, respectively, where e is the eccentricity.

$$F_1 = -\frac{2}{3} P_1 \ell_a \int_0^{2\pi} \frac{(c'+e\cos\theta)^3 \cos\theta\, d\theta}{\{(c'+e\cos\theta)^3+(c+e\cos\theta)^3\}}$$

The part of the piston to the right of the groove is shown with tentative dimensions. At the groove, the pressure is $2/3P_s$ and at the cap end it drops to atmospheric pressure. Computations of the net lateral force can be made similar to that for the left part. The governing equation still remains

$dp/d\theta = -12\mu/y^3 dQ/dz.$

If $p_g$ is the pressure at the groove and P is the pressure at any intermediate point x from the groove, then

$P-P_g = -12\mu dQ/dz \int dx/y^3.$

Once again clearance y is a function of x and also of angle $\theta$. Assuming the clearance to be c and $c_1$ for $0<x<1$ and $1<x<3.11$, respectively, and if location of x falls between 1 and 3.11, then

$$P-P_g = -12\mu dQ/dz\left[\int_0^{\ell} dx/c^3+\int_{\ell}^{x} dx/{c_1}^3\right]$$

The boundary conditions at $x = 3.11$ is $P = P_2 = 0$, giving

i.e. $P = P_g-P_g/(2.1c^3+{c_1}^3)\{(x-1)c^3+1{c_1}^3\}$

Integrating the pressure to get a radial force

acting on an elementry strip of width dz gives

$$\frac{dF}{dz} = 3.1\ Pg\ell - \frac{3.1\ell Pg\ c'^3}{(c'^3+2.1c^3)} - \frac{(1.7\ell)Pgc^3}{(c'^3+2.1c^3)}$$

Integrating the above equation and considering only the vertical components, the net lateral force is

$$F_2 = -3.1Pg\ell a\int_0^{2\pi} \frac{(c'+e\cos\theta)\cos\theta\ d\theta}{(c'+e\cos\theta)^3+2.1(c'+e\cos\theta)^3} - 1.7\ell aPg\int_0^{2\pi} \frac{(c + e\cos\theta)^3\ \cos\theta\ d\theta}{(c'+e\cos\theta)^3+2.1(c+e\cos\theta)} \qquad \text{B.6}$$

The net lateral force on such a stepped piston would be sum of the above two forces. Detailed computations for lateral forces was made for $1<c/c_1<2.5$ and $0<e/c_1<1$. These numbers do not correspond to any particular machine; they are roughly what might be expected from any machine with modest design criteria and practical limitations. Using these values of $c/c_1$ and $e/c_1$, one gets a net force between 178 N and 266 N on each piston.

If as before the limiting case of contact with the wall is considered (i.e. b = c), the lateral force is which corresponds to an angle of 13 degrees between the cap force and the centerline of the cylinder. This is comparable to the result for the double-tapered design above. Thus the preferred choice is largely a matter of cost.

VITA

Parveen Kumar Gupta was born on 7th October 1955 in Ambala, India and is the second son of Mrs. Tara Devi and Mr. Vijay Kumar. He graduated from Institute of Technology, Banaras Hindu University in June 1978 with B.S in Mechanical Engineering(with honours). He then worked for Union Carbide as a Project Engineer untill December 1980. The author pursued graduate studies in Mechanical Engineering from June 1981 until May 1983. During this time the author performed research for this thesis.

TABLE 1

Raw Data Corrected for Instrument Calibration

| Sl.No | Pressure Gauge 1 Reading kPa | Pressure Gauge 2 Reading kPa | Pressure Gauge 3 Reading kPa | Pressure Gauge 4 Reading kPa | Return Flow 5 $m^3/s*10^{-5}$ | Drain Flow 6 $m^3/s*10^{-5}$ | Load Flow $m^3/s*10^{-5}$ | No. of turns from zero location (clockwise) |
|---|---|---|---|---|---|---|---|---|
| 1 | 2346 | 19.55 | 1828.5 | 2484 | 19.55 | 1.19 | 4.43 | 5 |
| 2 | 3243 | 17.42 | 2691.1 | 7831.5 | 17.42 | 1.51 | 4.10 | 5 |
| 3 | 3519 | 11.18 | 3036 | 11,626.5 | 11.18 | 1.58 | 2.52 | 5 |
| 4 | 3036 | 72.45 | 3174 | 6003 | 6.98 | 1.77 | 4.73 | 10 |
| 5 | 3105 | 300.2 | 3036 | 3691.5 | 17.7 | 1.89 | 10.73 | 10 |
| 6 | 3312 | 165.6 | 3208.5 | 6072 | 12.76 | 1.956 | 7.57 | 10 |
| 7 | 3588 | 100.05 | 3415.5 | 7210.5 | 9.04 | 1.956 | 5.36 | 10 |
| 8 | 3657 | 61.5 | 3519 | 7590 | 6.98 | 1.77 | 4.42 | 10 |
| 9 | 3243 | 179.4 | 3036 | 3174 | 12.29 | 1.58 | 11.99 | 15 |
| 10 | 3657 | 93.15 | 3381 | 5175 | 8.85 | 1.64 | 8.52 | 15 |
| 11 | 3657 | 44.85 | 3588 | 5865 | 4.84 | 1.64 | 5.05 | 20 |
| 12 | 3657 | 72.45 | 3208.5 | 4105.5 | 6.98 | 1.58 | 9.78 | 20 |
| 13 | 3657 | 39.67 | 3588 | 4588.5 | 5.12 | 1.58 | 6.63 | 20 |
| 14 | 3726 | 27.6 | 3657 | 4795.5 | 3.90 | 1.58 | 4.73 | 20 |
| 15 | 3105 | 97.9 | 3105 | 3312 | 3.07 | 1.77 | 5.05 | 23 |

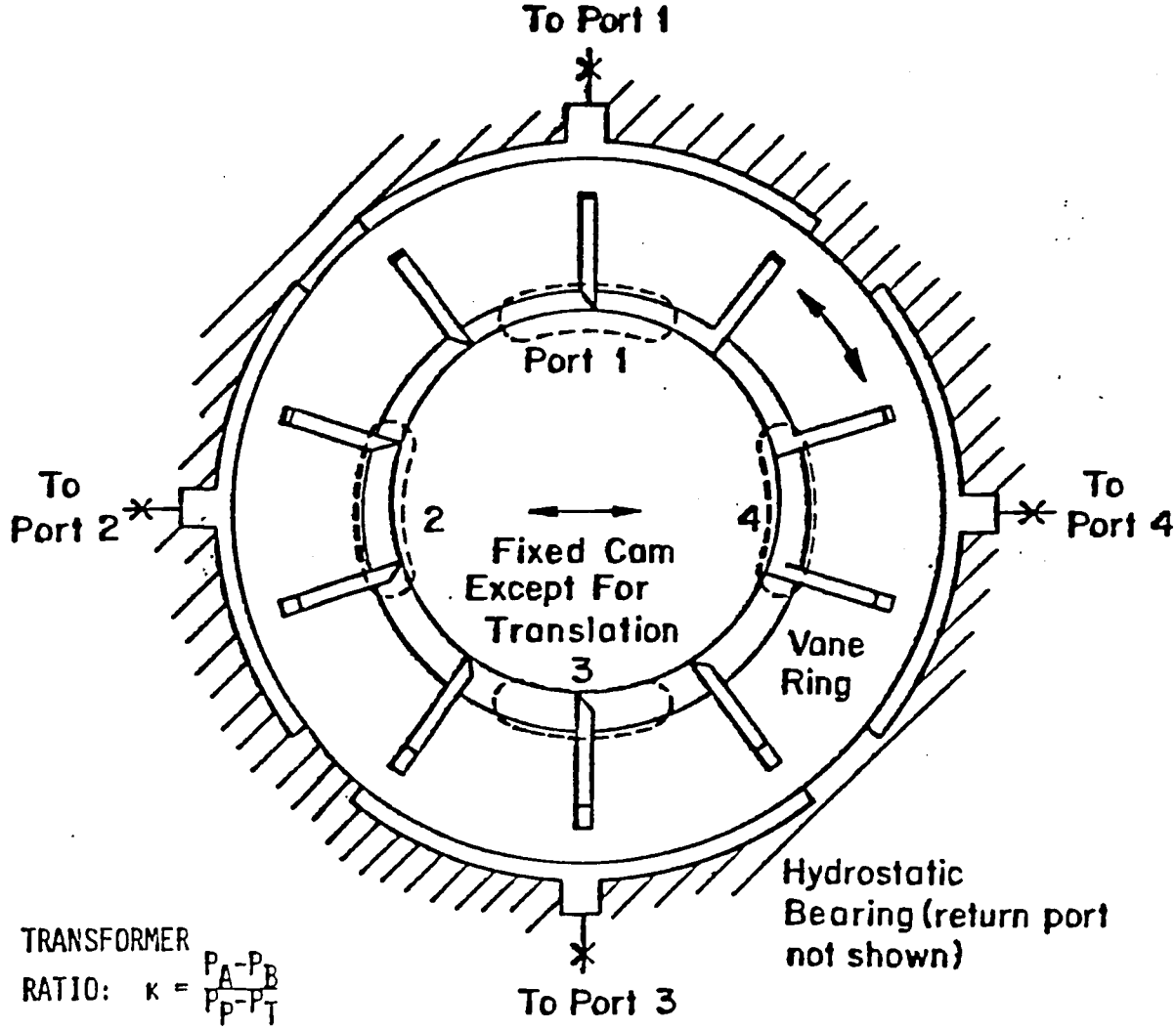


POSSIBLE PORTINGS - P = PUMP, T = TANK, A,B ACROSS LOAD:

| # | PORT 1 | PORT 2 | PORT 3 | PORT 4 | $x > 0$ | $x < 0$ |
|---|---|---|---|---|---|---|
| 1 | P | A | T | B | $-1 < \kappa < 0$ | $0 < \kappa < 1$ |
| 2 | B | T | A | P | $-\infty < \kappa < -1$ | $1 < \kappa < \infty$ |
| 3 | T | B | P | A | $-1 < \kappa < 0$ | $0 < \kappa < 1$ |
| 4 | A | P | B | T | $-\infty < \kappa < -1$ | $1 < \kappa < \infty$ |

Fig. 1 Vane Wheel Concept

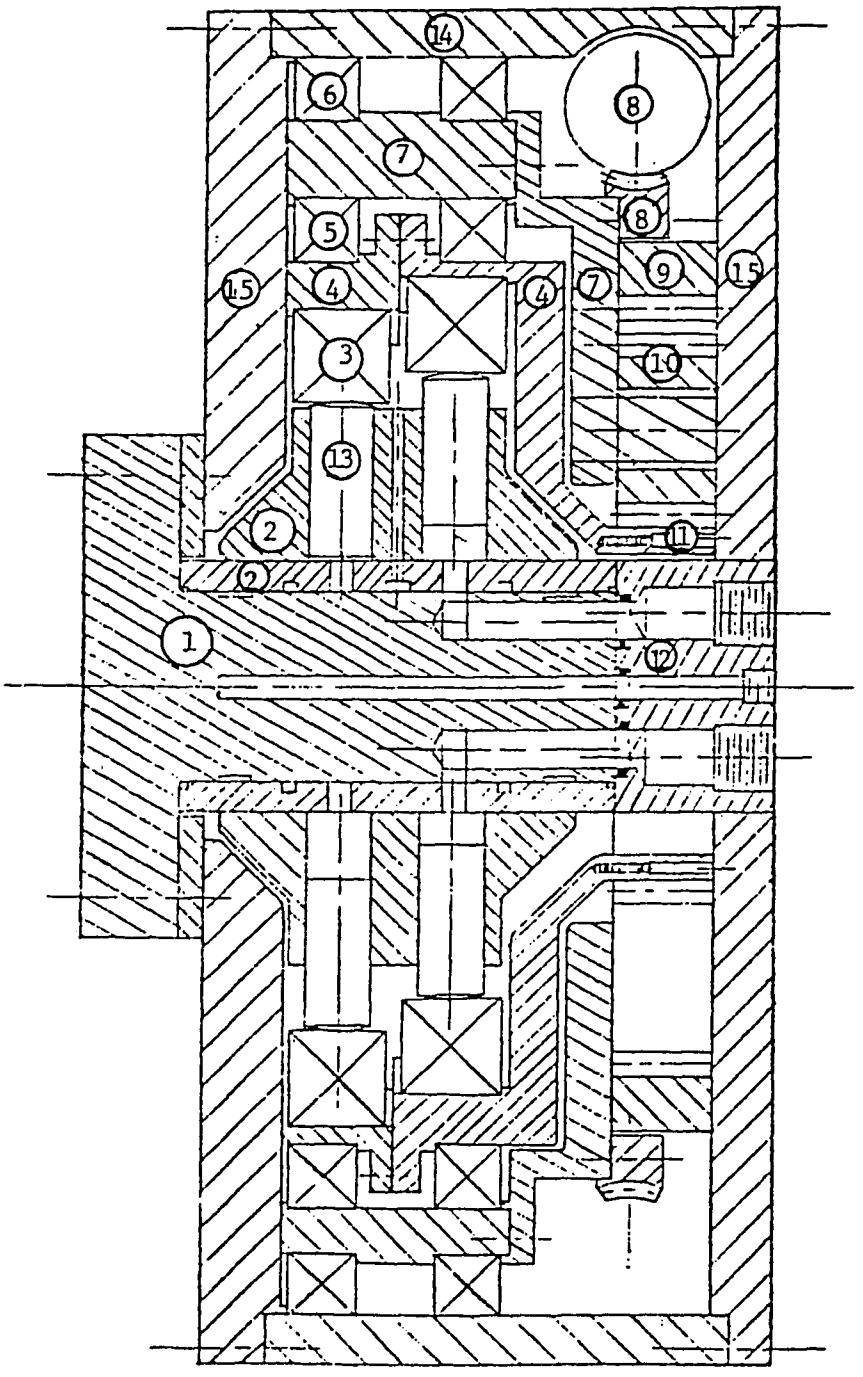


Fig. 2 Assembly Drawing of MHT

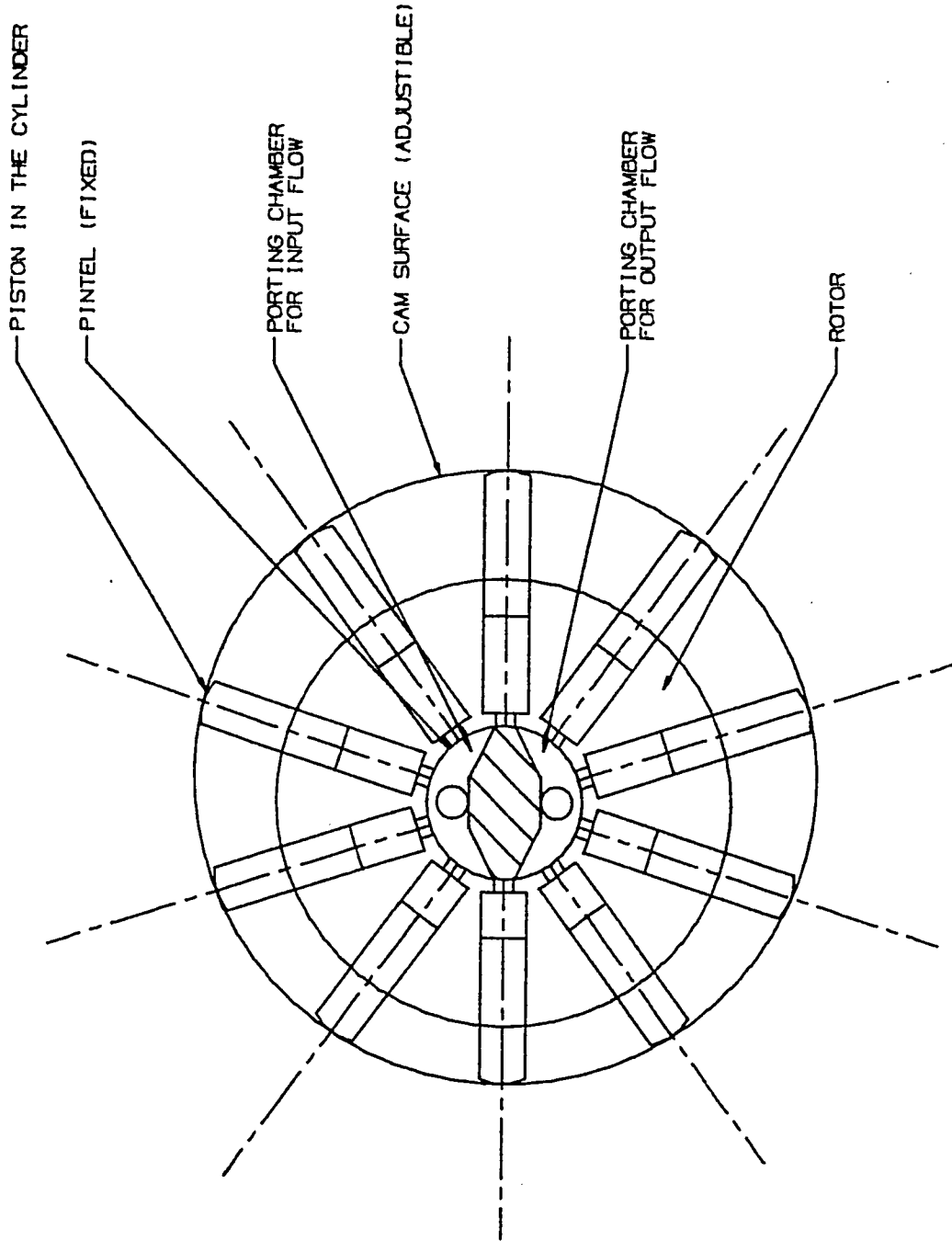


Note: The diameters of rotor and cam surface not to scale

Fig. 3 Configuration of Radial Piston Pump/Motor

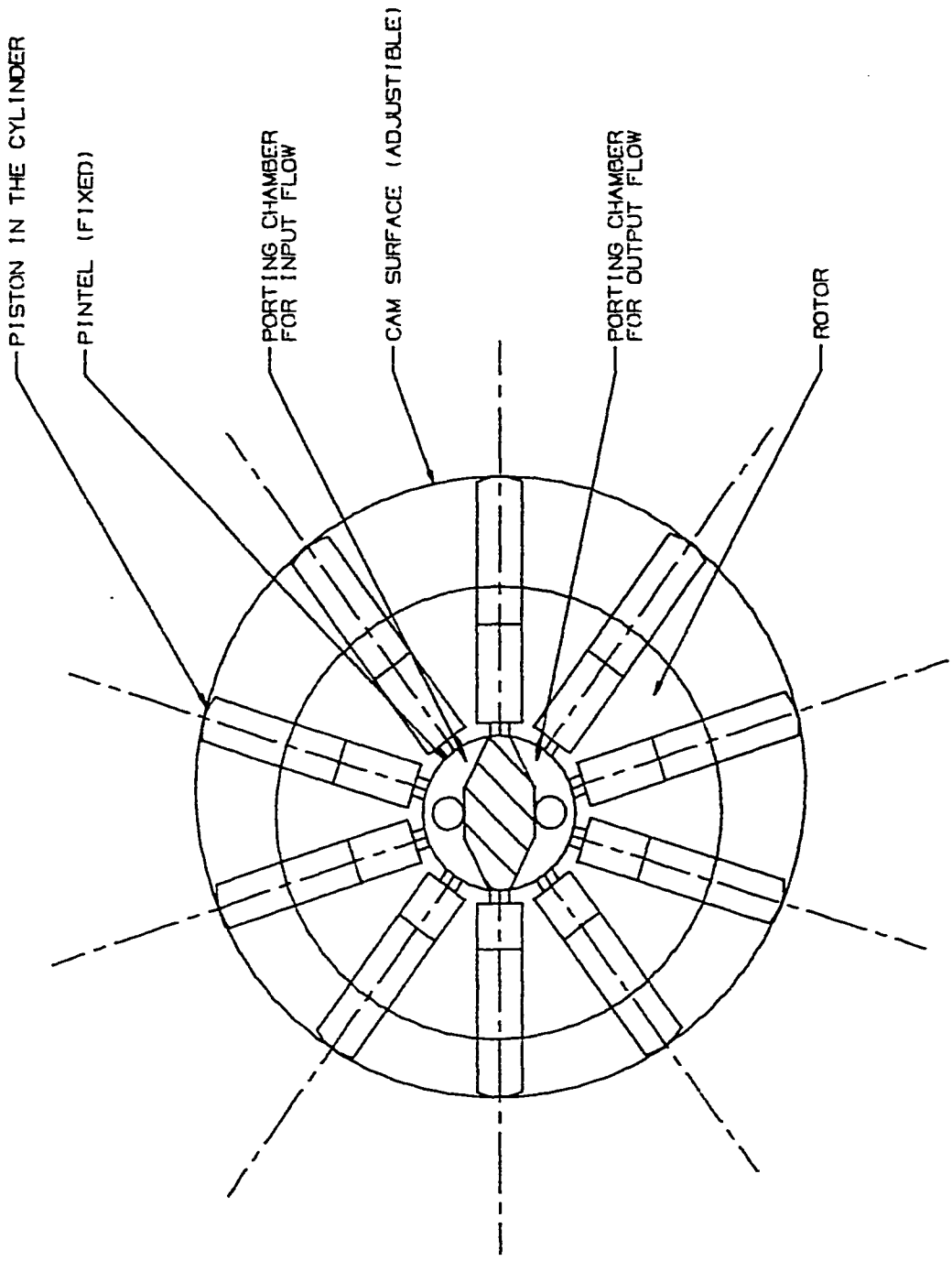


Note: The diameters of rotor and cam surface not to scale

Fig. 3 Configuration of Radial Piston Pump/Motor

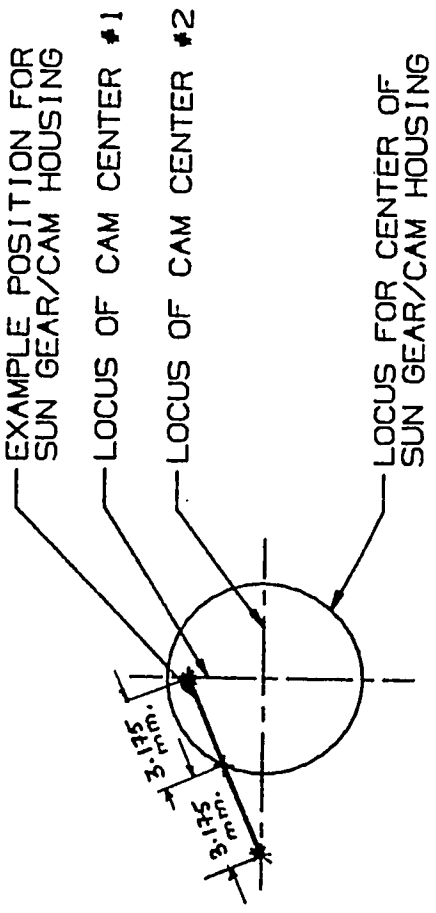


Fig. 4 Concept of Cam Housing/Sun Gear Motion

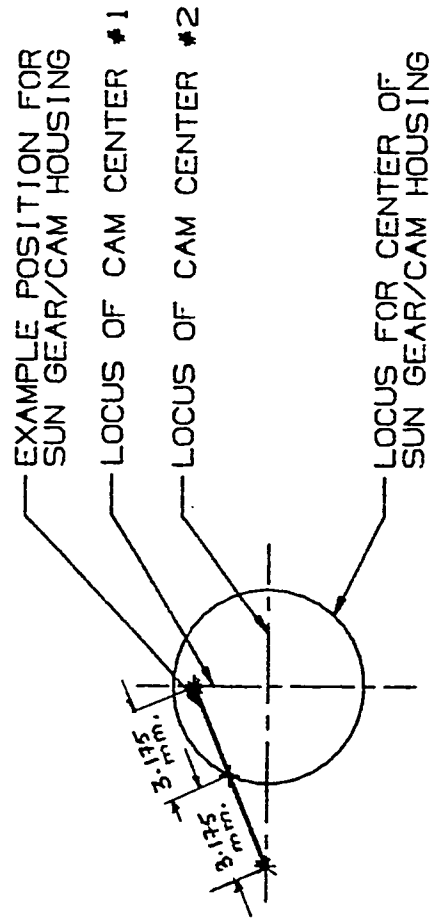


Fig. 4 Concept of Cam Housing/Sun Gear Motion

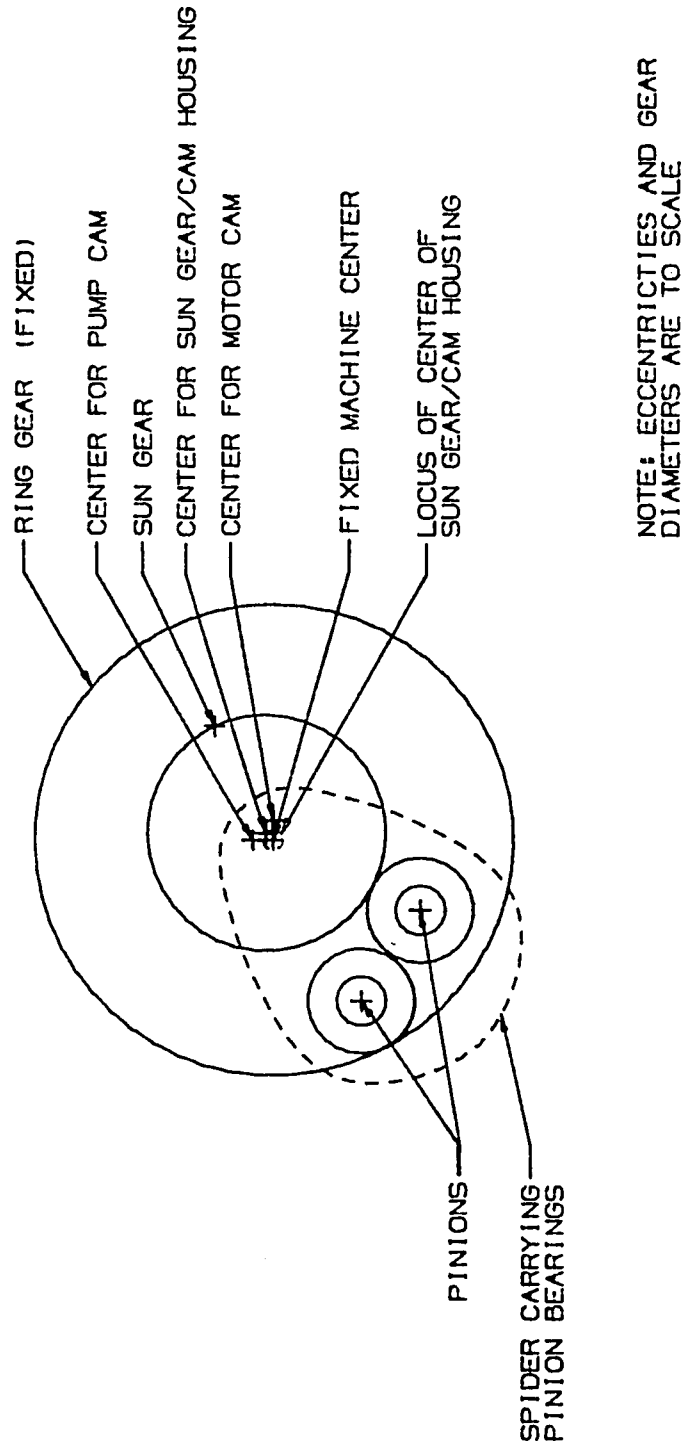


Fig. 5 Schematic for Epicyclic Modulation of Cam Housing

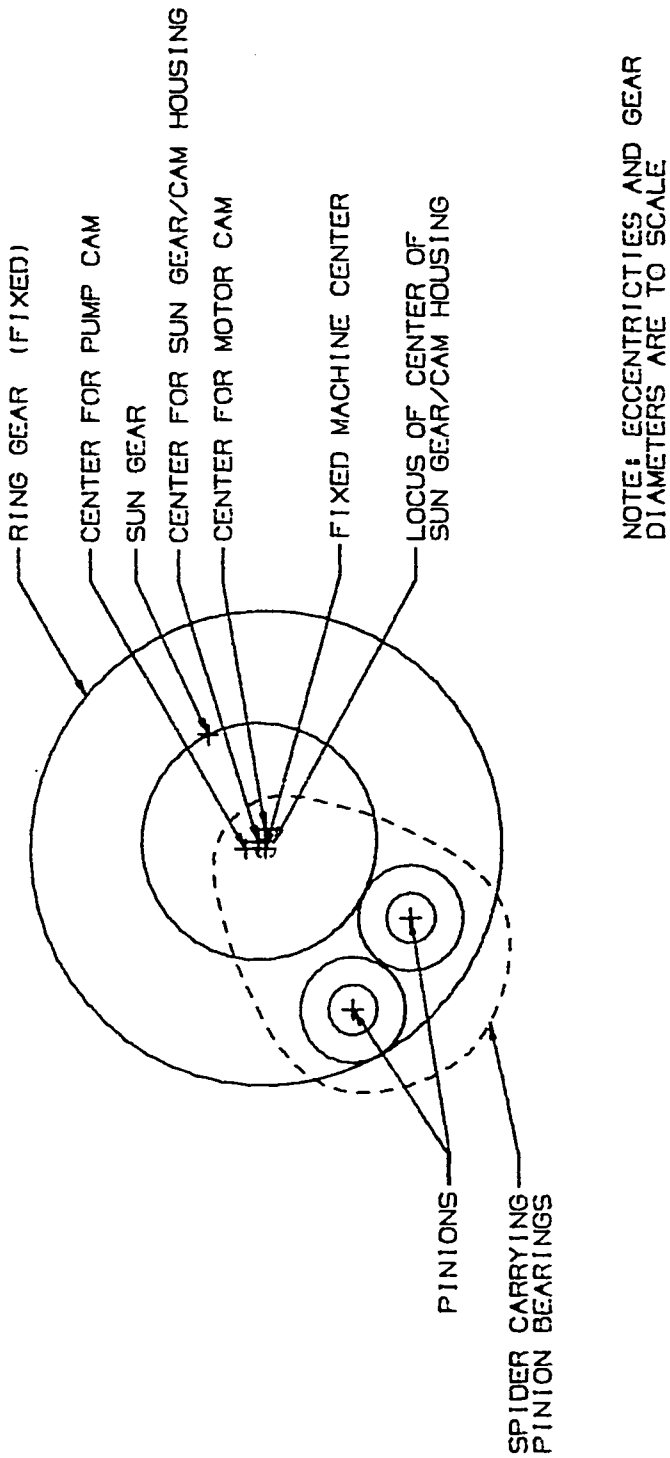


Fig. 5 Schematic for Epicyclic Modulation of Cam Housing

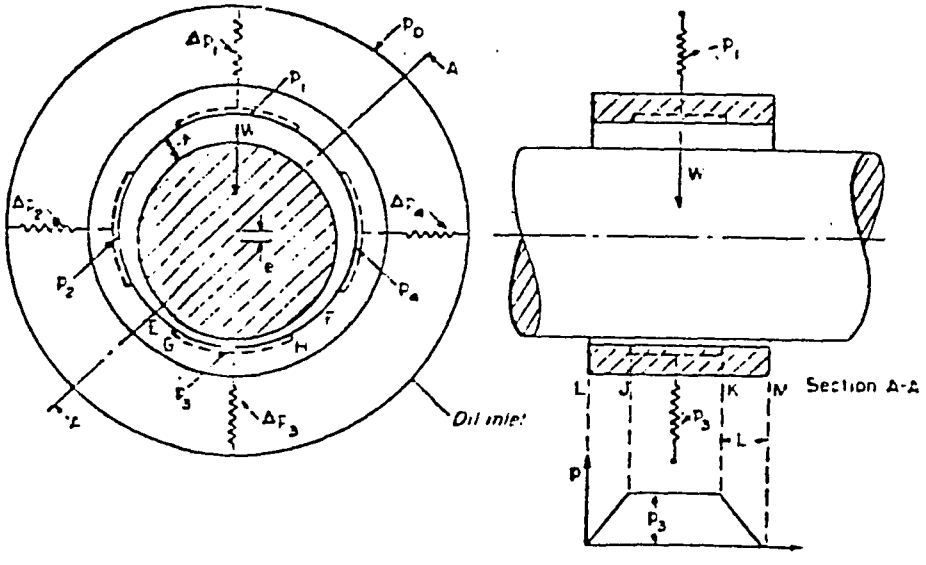


Fig. 6 Externally Pressurized Journal Bearing with Four External Resistances

Source: Fig. 7.39 of Reference [1]

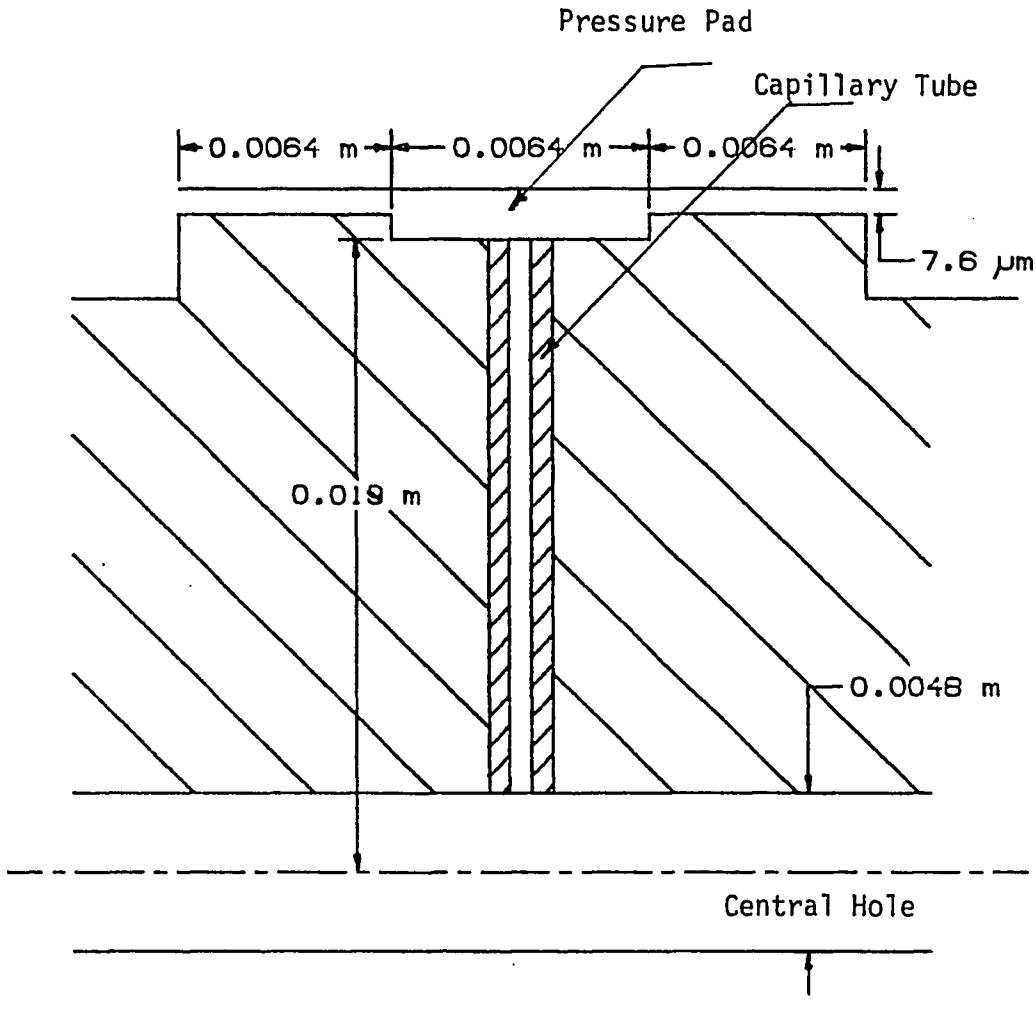


Fig. 7 Cross Section of Hydrostatic Bearing Through a Capillary Tube

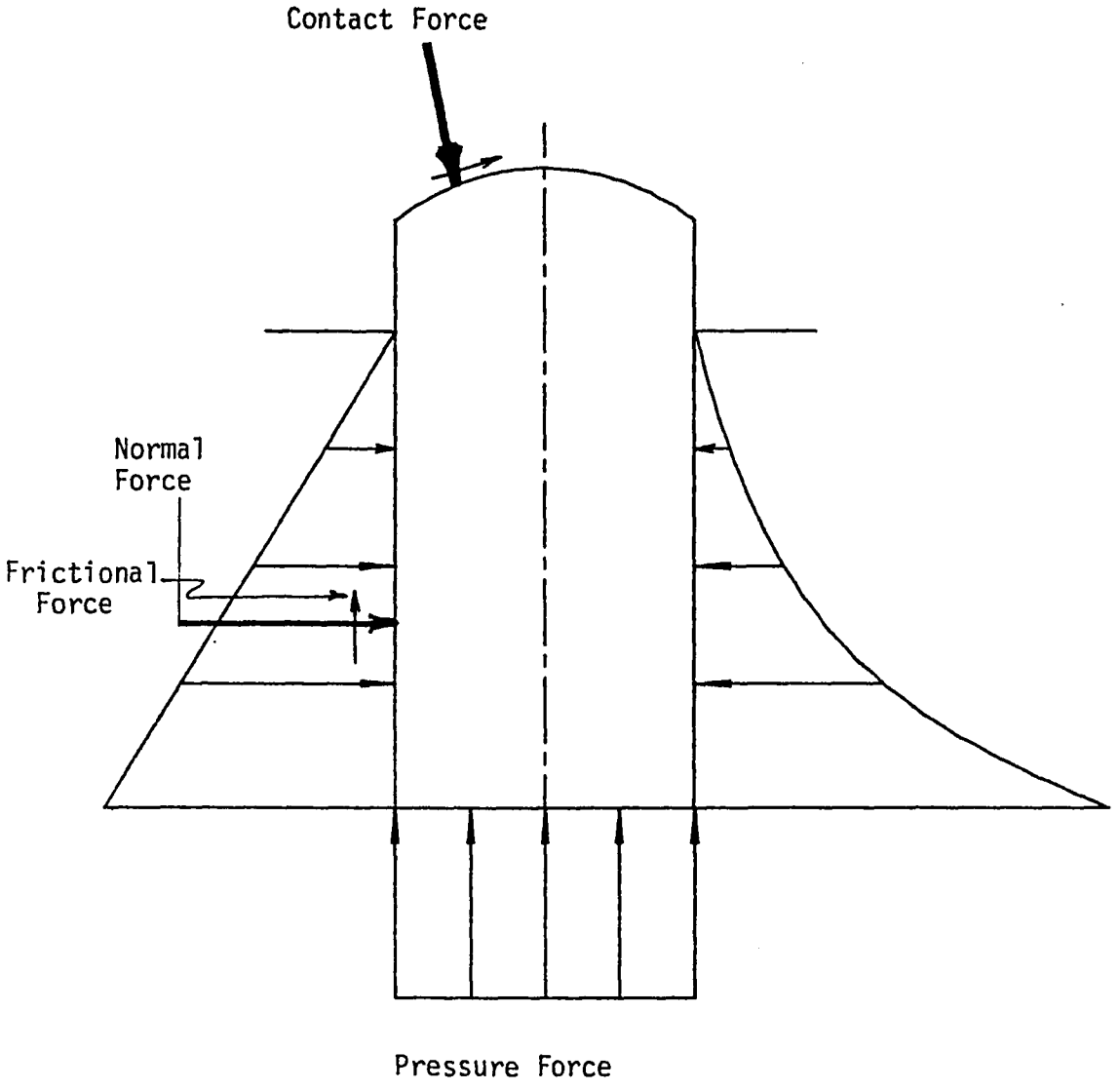


Fig. 8 Forces on Cylindrical Piston

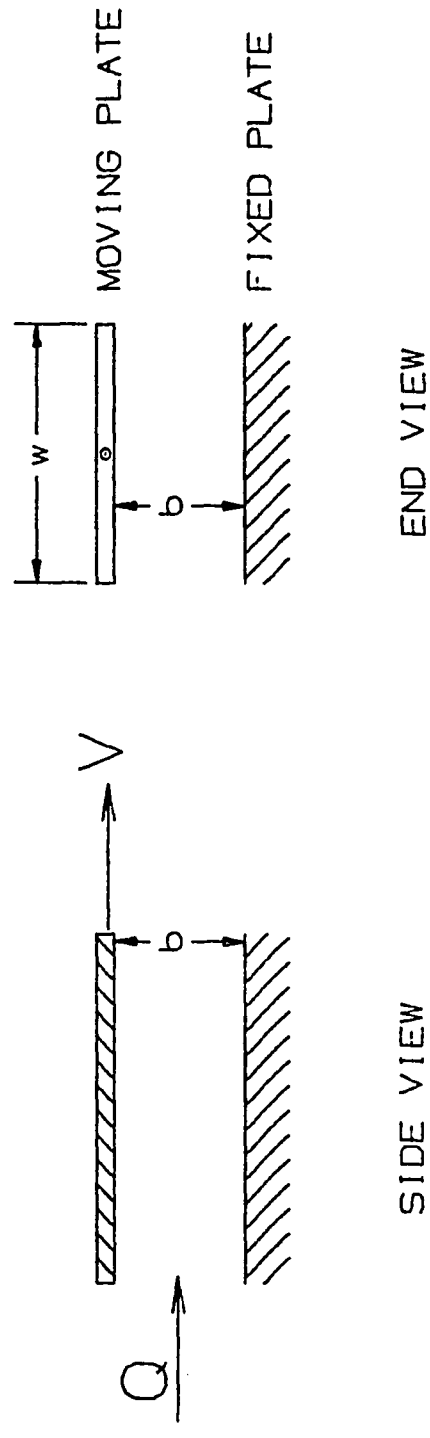


Fig. 9 Relative Motion Between Fixed and Moving Plate

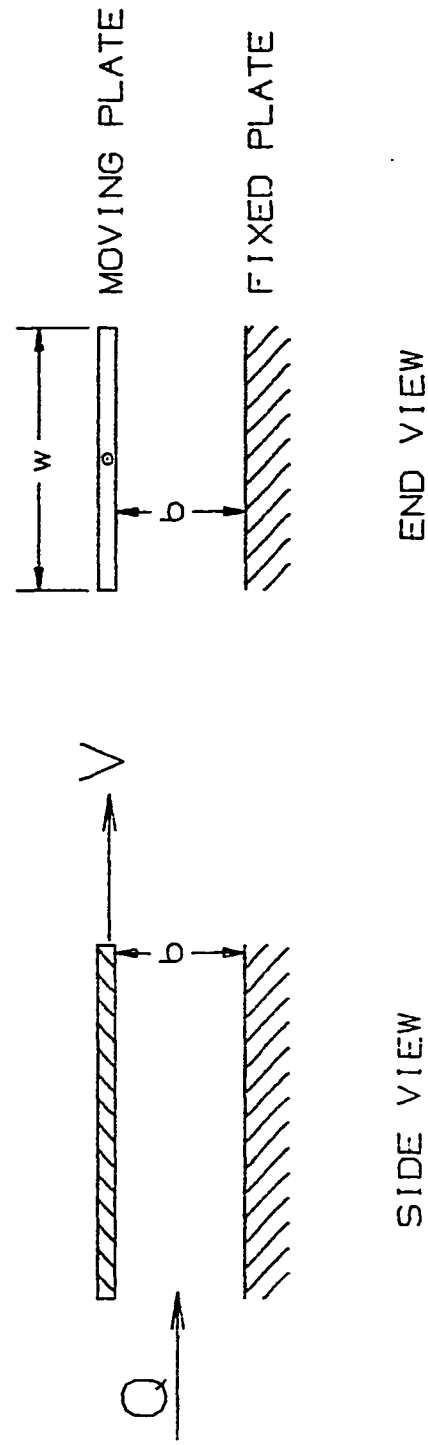


Fig. 9 Relative Motion Between Fixed and Moving Plate

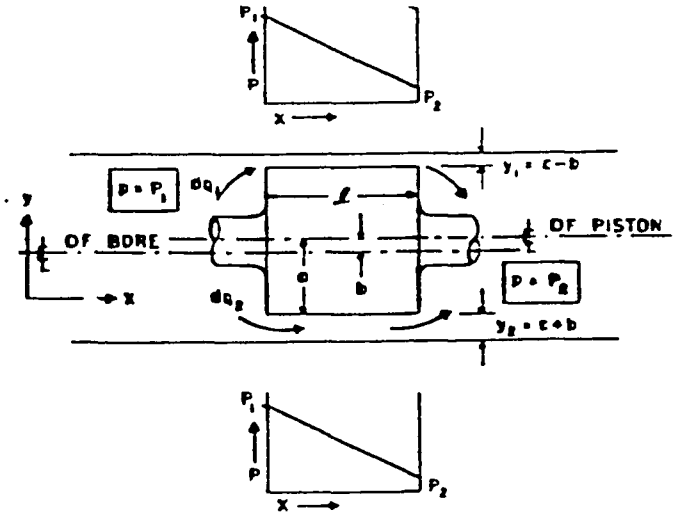


Fig. 10 Cylindrical Decenteres Piston

Source: Fig. 10.1 of Reference [1]

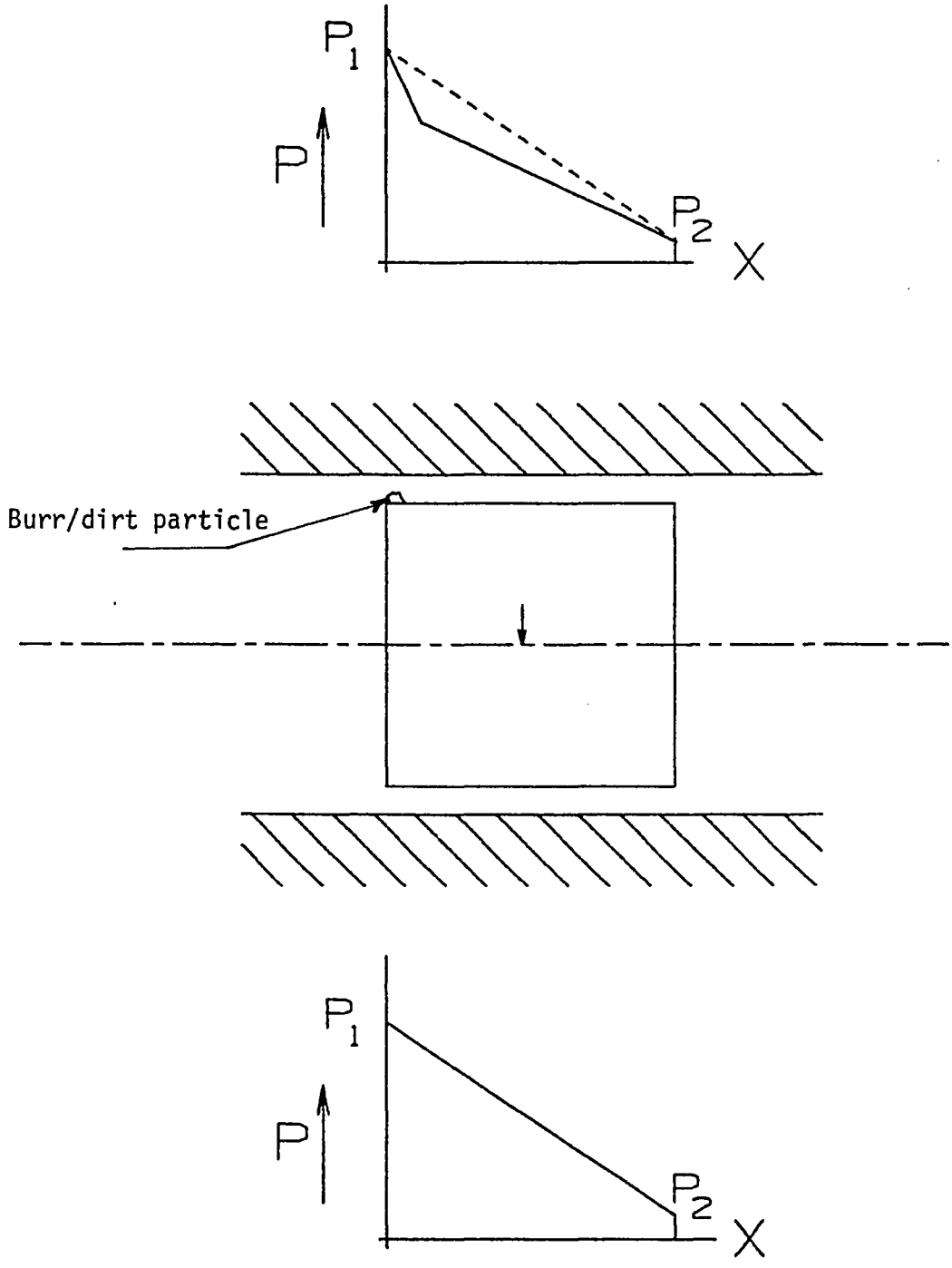


Fig. 11 Forces on Cylindrical Piston with Burr/Dirt Particle

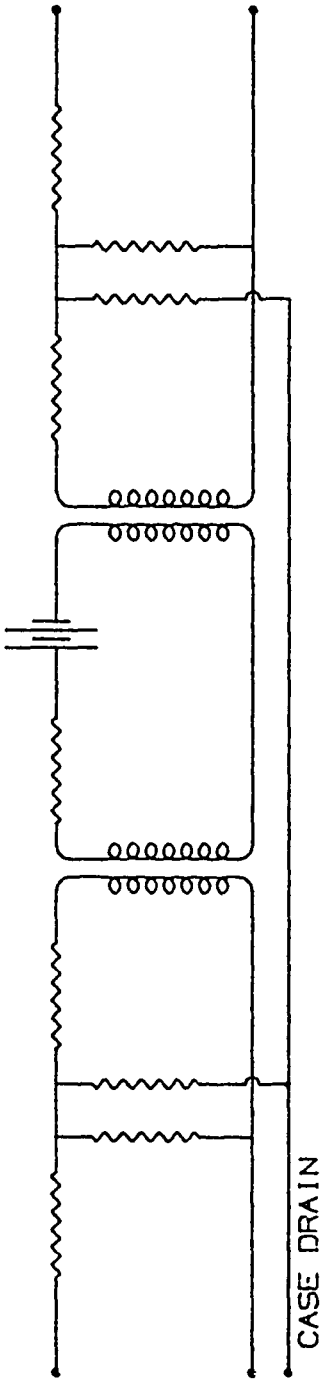


Fig. 12a Circuit Model of MHT

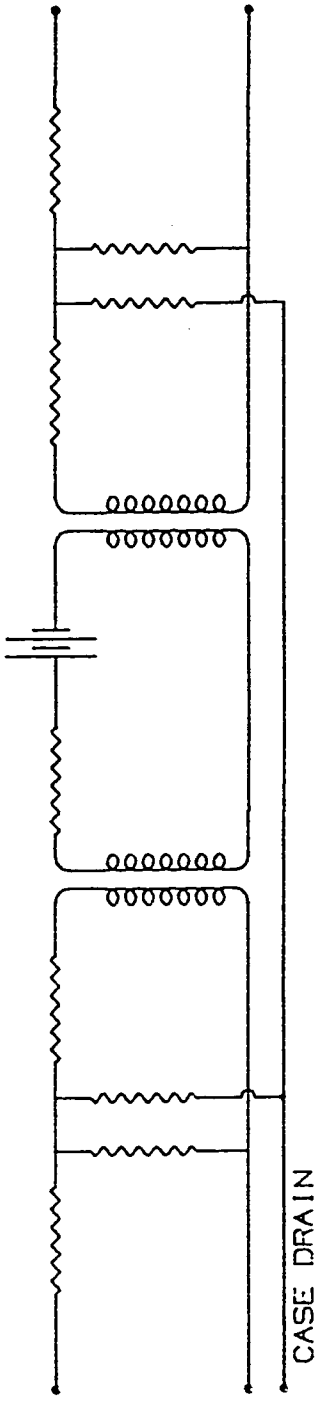


Fig. 12a Circuit Model of MHT

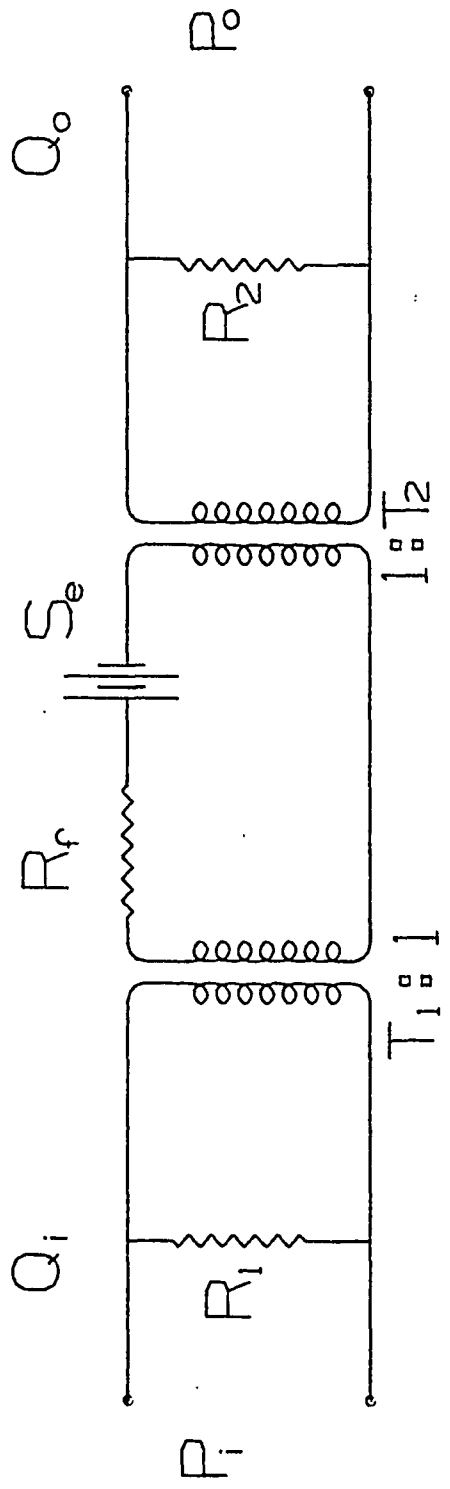


Fig. 12b Simplified Circuit Model of MHT

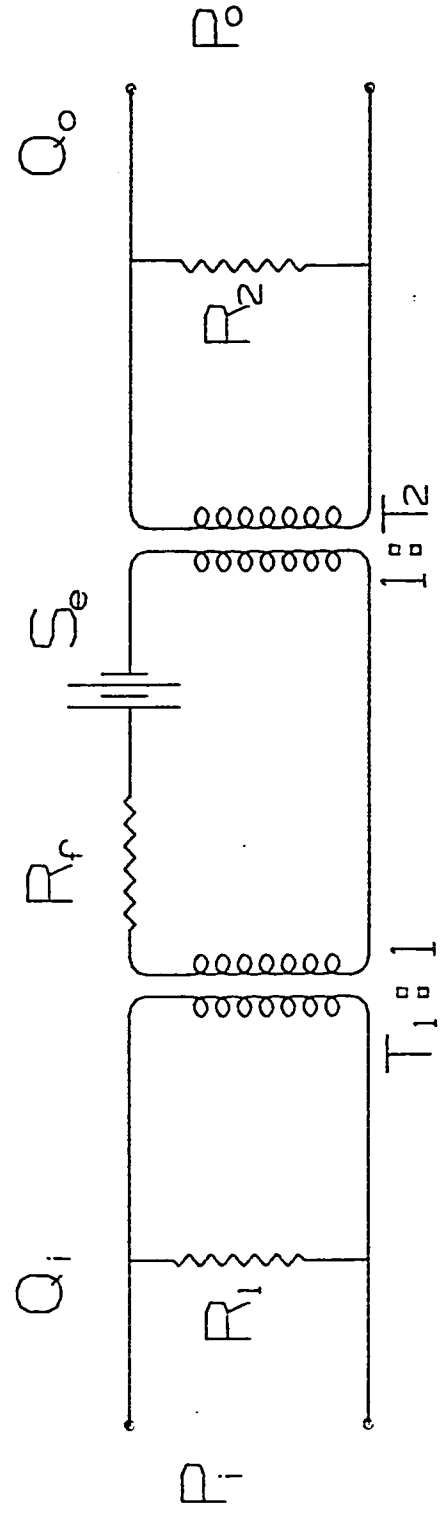


Fig. 12b Simplified Circuit Model of MHT

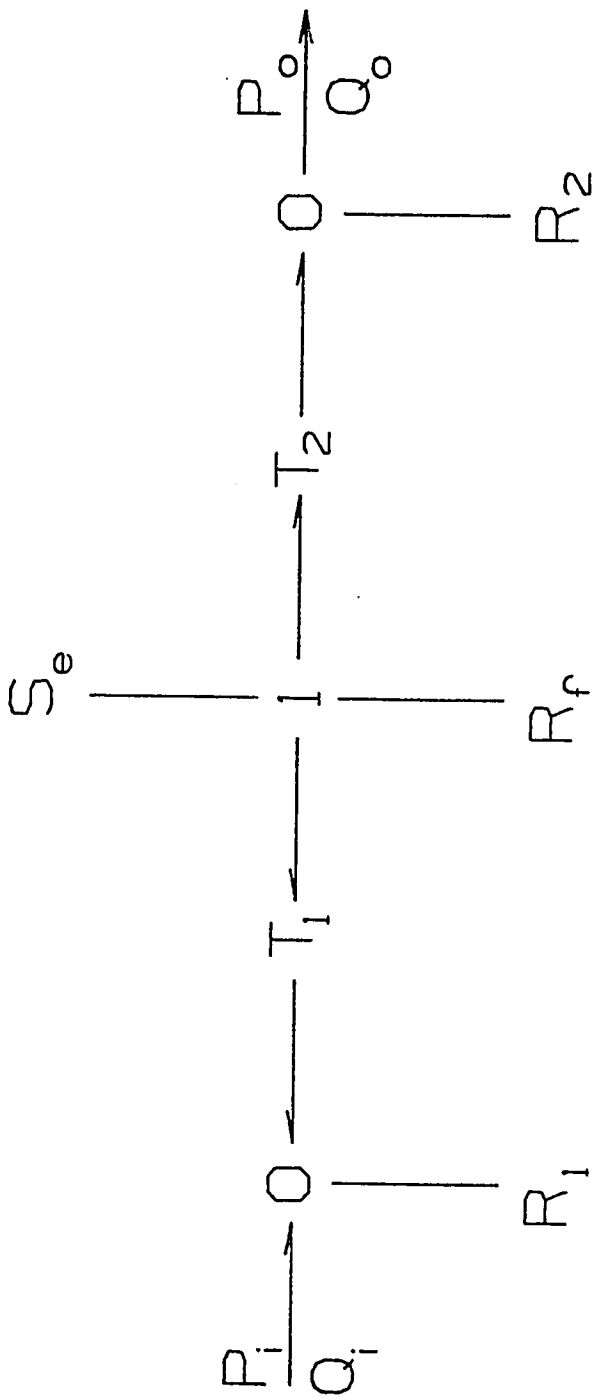


Fig. 12C Bond Graph for MHT

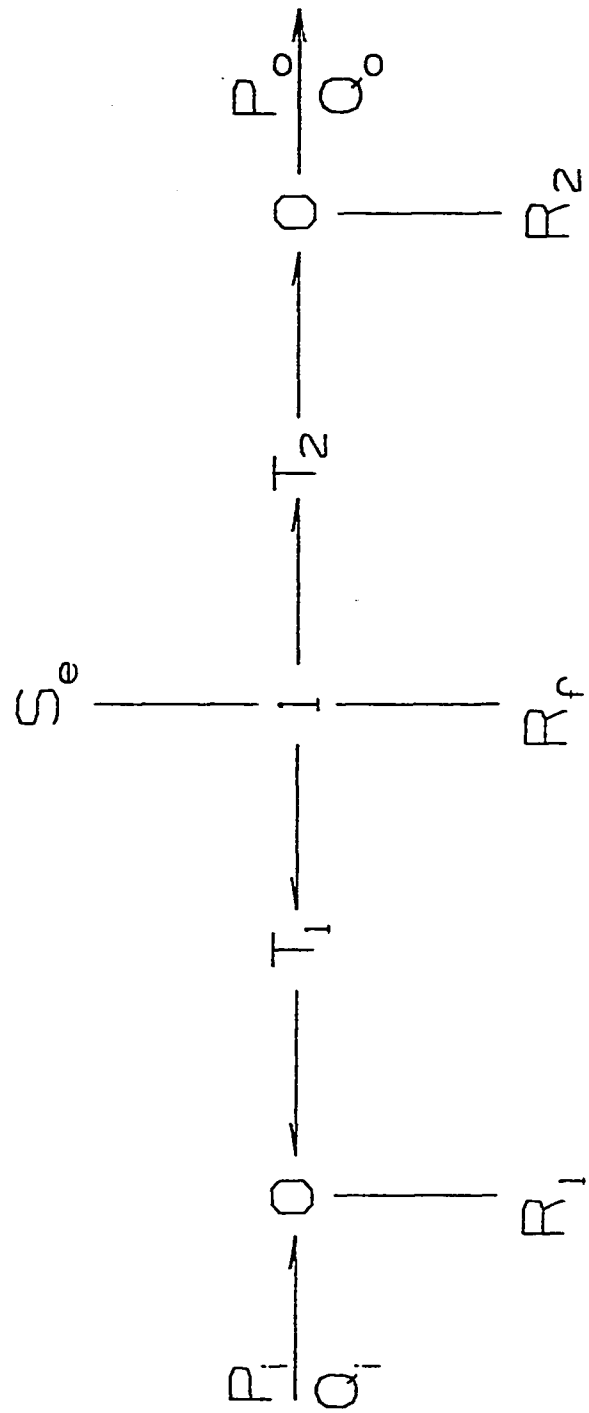


Fig. 12C Bond Graph for MHT

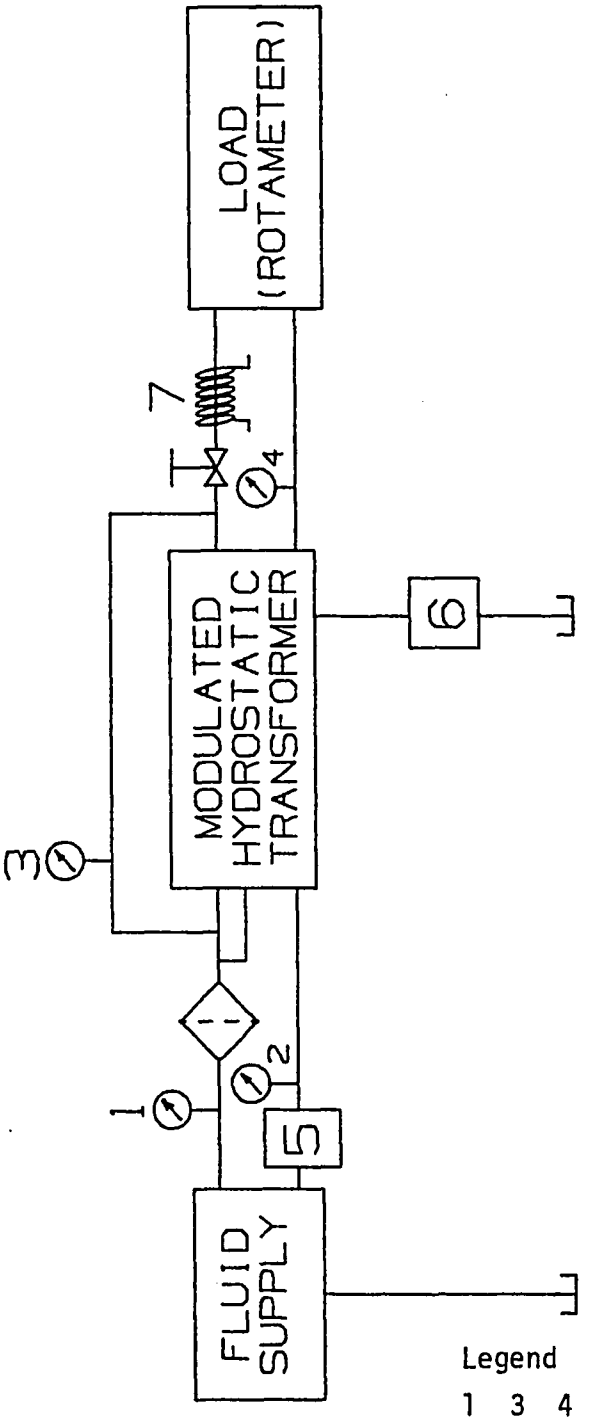


Legend

| | |
|---|---|
| 1 3 4 | Higher Pressure Range pressure gauges (1-2000 psi) |
| 2 | Low Pressure Range pressure gauge (0-60 psi) |
| 5 6 | Rotameters |
| 7 | Heat Exchanger |

Fig. 13 Schematic for Experimental Set-up for MHT

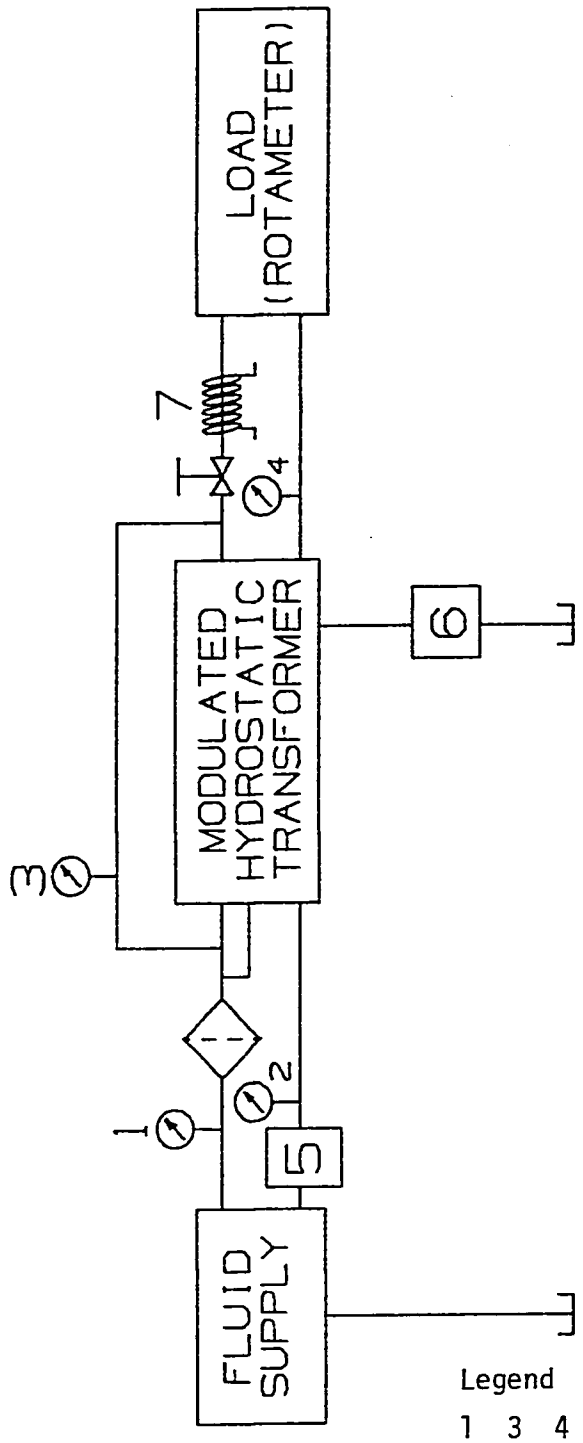


Legend

| | |
|---|---|
| 1 3 4 | Higher Pressure Range pressure gauges (1-2000 psi) |
| 2 | Low Pressure Range pressure gauge (0-60 psi) |
| 5 6 | Rotameters |
| 7 | Heat Exchanger |

Fig. 13 Schematic for Experimental Set-up for MHT

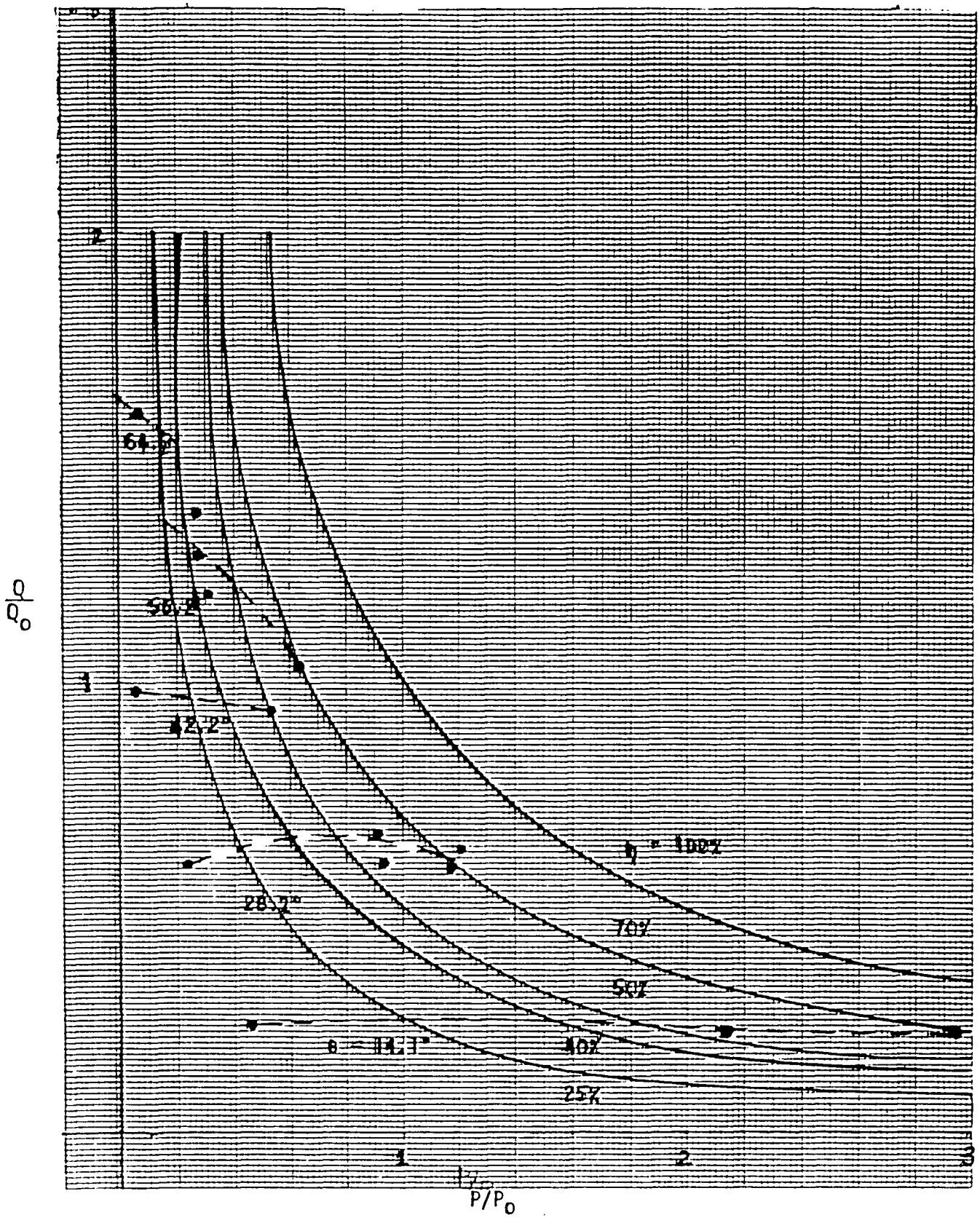


Fig. 14 Experimental Results of MHT

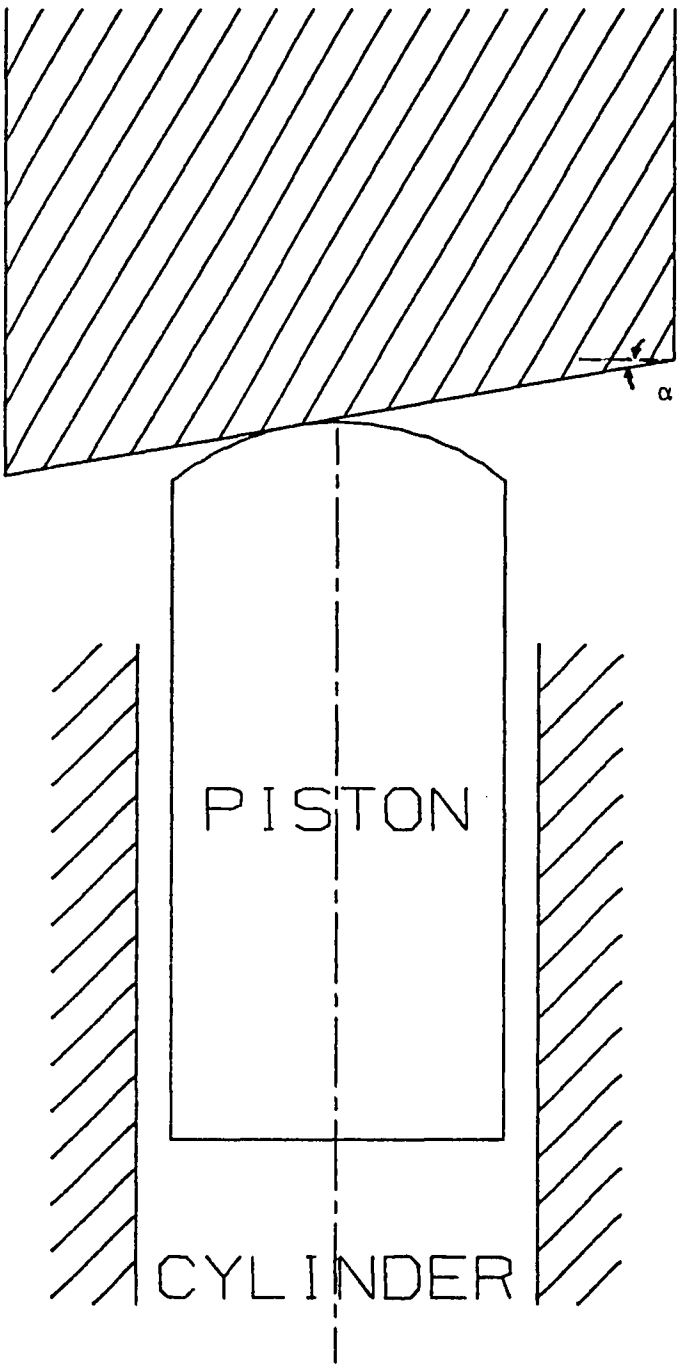


Fig. 15 Concept of Tapered Bearing

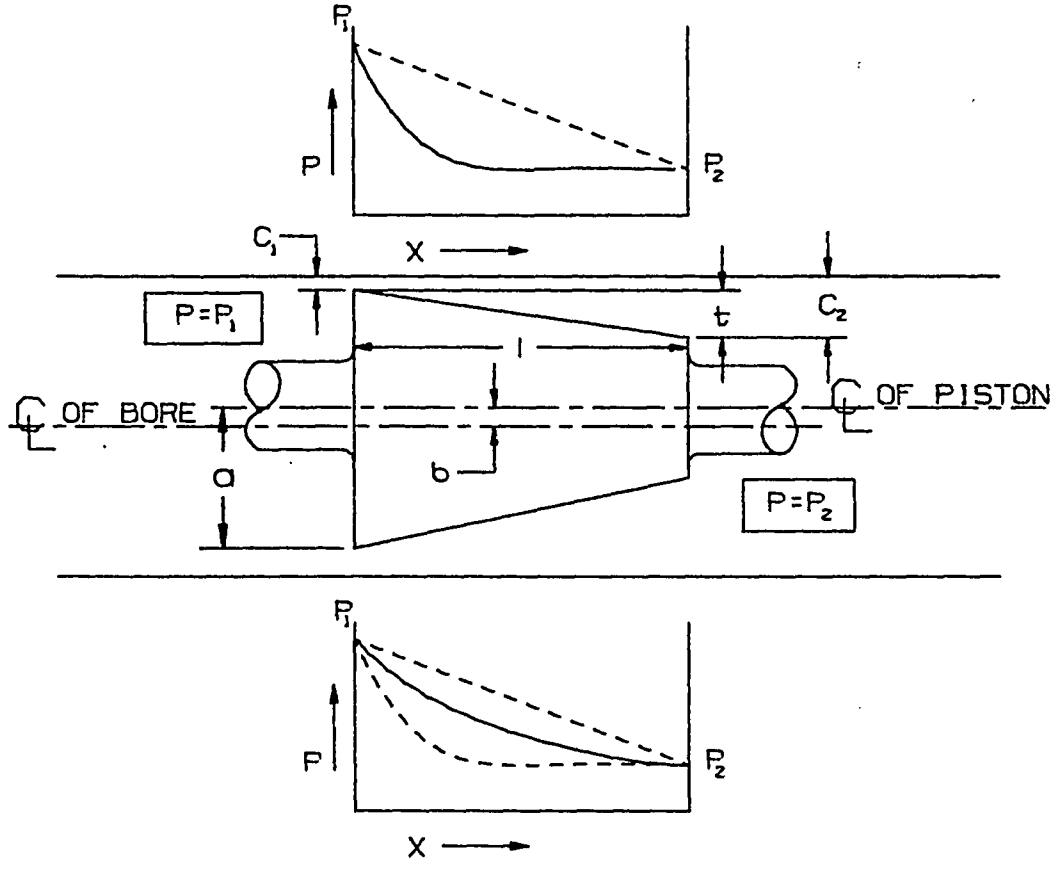


Fig. 16 Decentered Conical Piston

Source: Fig. 10.2 of Reference [1]

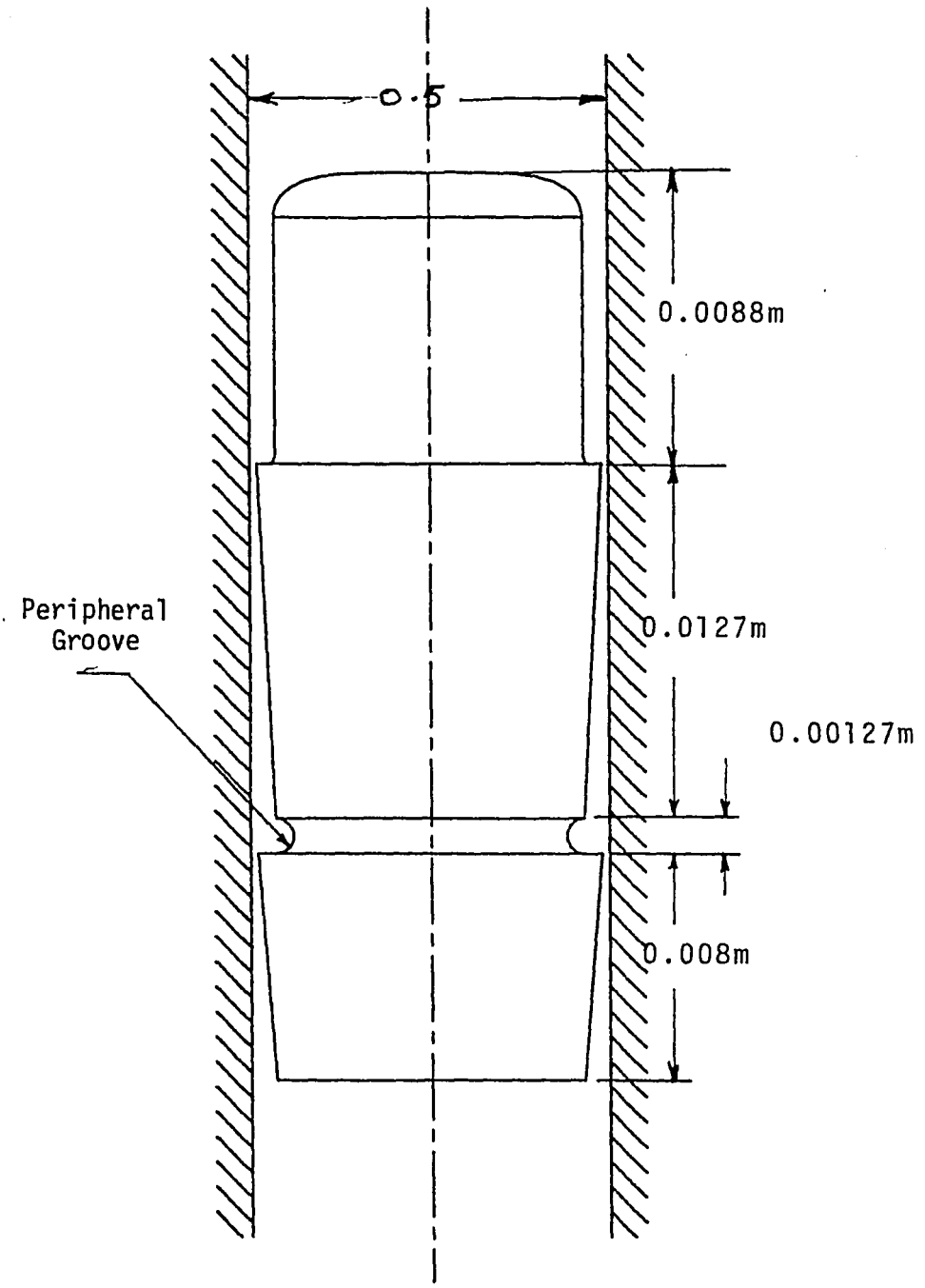


Fig. 17 Double Tapered Piston

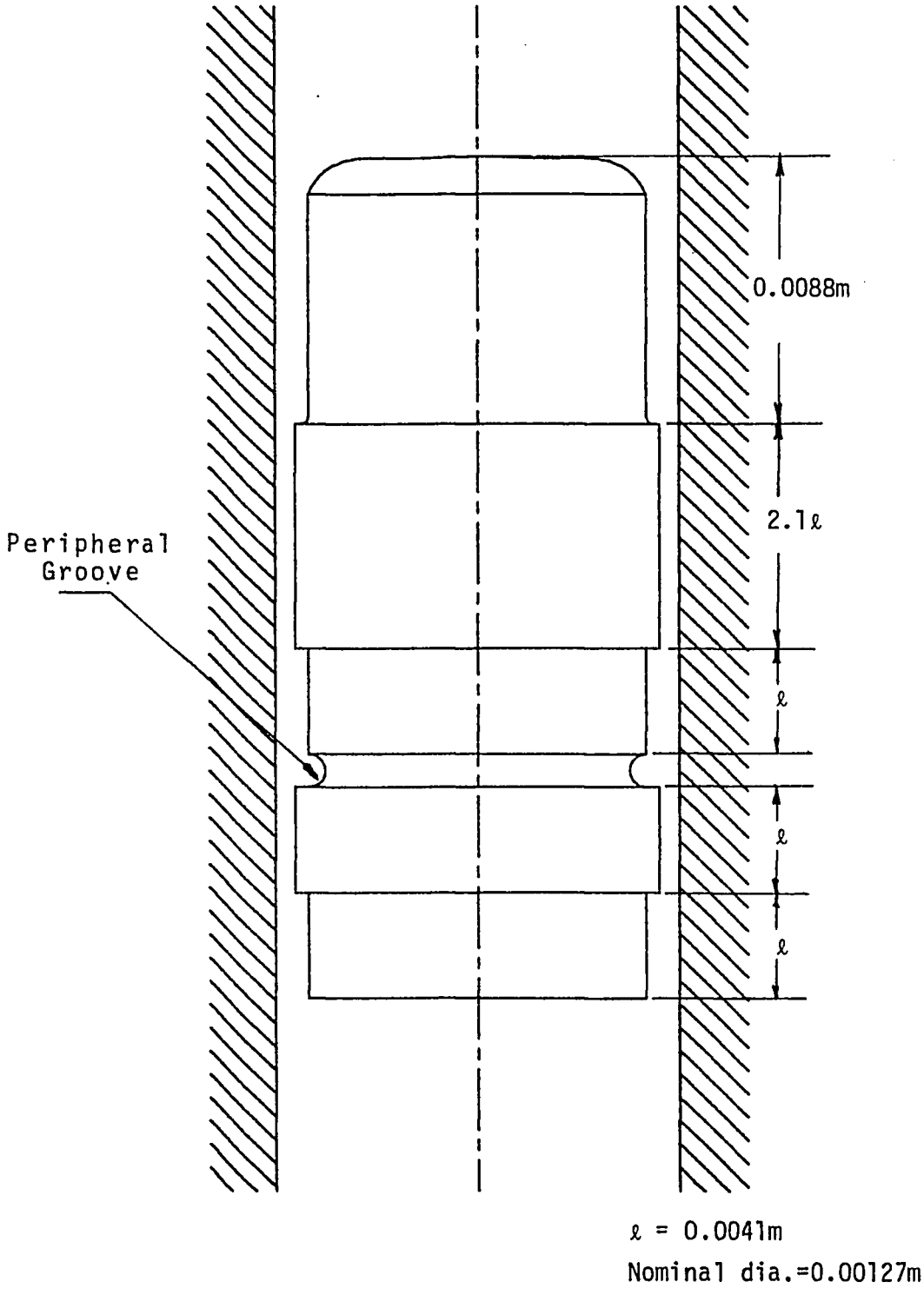


Fig. 18 Stepped Piston